ORIGINAL

NAL PROPOSAL No. 69

Correspondent: J. Lach
Experimental Facilities
National Accelerator Lab
Batavia, Ill. 60510

FTS/Commercial 312-231-6600 Ext. 453

ELASTIC SCATTERING OF THE HADRONS

M. Atac, C. Dolnick, P. Gollon, J. Lach,
J. MacLachlan, A. Roberts, R. Stefanski, D. Theriot
National Accelerator Laboratory

H. Kraybill, J. Marx, J. Sandweiss, W. Willis
Yale University

June 15, 1970

ELASTIC SCATTERING OF THE HADRONS

We propose to measure the elastic scattering of the hyperons Σ^-, Ξ^-, Ω^- and Λ^0 as well as the charged hadrons $\pi^\pm$, $K^\pm$, p and $\bar{p}$ over a region of momentum transfer up to about 1 GeV/c. For the more stable particles special attention will be given to the Coulomb interference region. As part of this program we will measure the production cross sections of the negative and positive hyperons and carry out a search for new particles with lifetime $\gtrsim 10^{-11}$ seconds. This experimental program is based on the use of novel detectors of high spatial resolution which we have developed.

M. Atac, C. Dolnick, P. Gollon, J. Lach, J. MacLachlan,
A. Roberts, R. Stefanski, and D. Theriot
National Accelerator Laboratory

H. Kraybill, J. Marx, J. Sandweiss, and W. Willis
Yale University

June 15, 1970

Correspondent: J. Lach

I. INTRODUCTION

We propose to measure the small angle scattering of essentially all the stable and quasi-stable charged particles. For some time we have been developing detectors of high spatial resolution - almost an order of magnitude greater than that obtained in normal wire spark chambers - necessary to do experiments with beams of high energy hyperons. While these detectors are essential for these experiments, because of the short lifetime of the hyperons, they offer tremendous advantages of convenience and economy when applied to the small angle scattering of the stable particles. For an experiment with a fixed momentum transfer acceptance, the weight of analyzing magnets can be reduced by one to two orders of magnitude, with a corresponding decrease in the space occupied by the apparatus.

These technical developments coincide well with our interest in the physics of small angle scattering: the change in shape or "shrinkage" as energy is increased; the measurement of the forward scattering amplitudes and comparison with SU3; the measurements of the real part of the forward scattering amplitude and thus the measurement of the total cross section by the optical theorem in a very clean way; and, especially, the application of these results to tests of the forward dispersion relations and the validity of relativistic quantum mechanics.

As part of this program we will measure the production cross section in the forward direction of the charged hyperons, Σ^-, Ξ^-, and Ω^-. The positive hyperons, Σ^+, $\overline{\Sigma}^+$, $\overline{\Xi}^+$, and $\overline{\Omega}^+$ will be produced along with a substantial proton flux, but we feel that those produced with substantial cross sections - as most likely the Σ^+ - can be detected and their production cross section measured. Two methods of detection are proposed to be implemented for the charged hyperons. One is a high resolution gas Cerenkov counter placed immediately after the magnetic channel and the

other relies on observing the hyperon decay products. We will be sensitive to hyperon decays which lead to a final state neutron such as

$$\Sigma^- \rightarrow n\pi^-$$

and to those which lead to a final state Λ^o such as

$$\Omega^- \rightarrow K^- \Lambda^o$$
$$\qquad\qquad\quad \lfloor \pi^- p$$

In addition, we are particularly interested in the search for new short lived particles, which might well escape discovery elsewhere. Also, the decay properties of such rare particles as the Ω^- will be studied very effectively.

While most of the effort will be devoted to charged particles, we hope to use the neutron-poor Λ beam created by Σ^- charge exchange in Be to study Λ-p scattering. This requires no additional equipment and is probably superior to experiments relying on direct neutral beams.

II. A. ENERGY DEPENDENCE OF SMALL ANGLE SCATTERING

In the last ten years this has been one of the topics in particle physics most discussed by theorists. Here we risk oversimplifying the issues to bring out what seems to be the most crucial question to be settled by going to high energy. This is whether the scattering of small momentum transfers approaches an energy dependent form as the energy increases, or continues to exhibit a steady shrinkage.

The different theories developed to explain elastic scattering divide rather clearly on this point. Theories of the Regge-pole type with a Pomeranchuk trajectory roughly parallel to other known trajectories predict a shrinking of the diffraction peak for all scattering processes, that is, a continuous increase of slope of the $d\sigma/dt$ as a function of energy. On the other hand, theories with a fixed Pomeranchuk singularity, that is a trajectory showing a very small slope increase with momentum transfer, as well as a wide class of theories related to the optical model such as that of Chou and Yang[1] or Durand and Lipes[2], predict an asymptotic approach to an elastic scattering differential cross section which is independent of energy, particularly at small $|t|$.

What we now know is that at AGS energies, some peaks shrink (p-p), some grow ($\bar{p}$-p), and some remain constant (π-p). Figure 1 illustrates this situation. The fashion among Regge theorists recently has been for a flat Pomeranchuk trajectory. The observed variations with energy are then ascribed to secondary trajectories, while effects at large $|t|$ are obscured by cuts. Thus the question can only be resolved by experiments at higher energy and at very small $|t|$. Great interest has been aroused by the only higher energy result available, the p-p scattering from Serpukhov. There

---

[1] T. T. Chou and C. N. Yang, Phys. Rev. 170, 1591 (1968).

[2] L. Durand and R. Lipes, Phys. Rev. Letters 20, 637 (1968).

it seems that the p-p elastic peak does not stop shrinking, but rather indicates a Pomeranchuk trajectory with a large slope, Fig. 2. If these results are really correct, perhaps we will find that at sufficiently high energies the π-p and $\bar{p}$-p peaks will begin to shrink too. If so, the old-fashioned Regge model may turn out to be right after all!

To answer these questions, we should determine the trajectory function, $\alpha(t)$, to an accuracy of 0.05-0.10 in bins of 0.1 in $-t^2$. This requires 10,000-20,000 events at each energy, if the determination is made on the basis of measurements at 75 GeV/c and 150 GeV/c. We would probably wish to take 4-6 different energies. For the rarer hyperons, where the rates are limited by flux, we would make do with smaller statistics, appropriate to the fluxes found in the experiment.

II. B. Re f(0) AND TOTAL CROSS SECTIONS

For the more stable particles (π, K, p) we propose to measure the forward scattering down to values of $|t| = 0.001$ (GeV/c)^2. This enables us to measure the real part of f(0) by observing the interference of the nuclear and coulomb amplitudes. These measurements extending on the high side to $|t| \cong 0.2$ or more allow a simultaneous determination of Re f(0), b and c, and σ_{tot} for the π-p and K-p interactions. The quantities b and c are the coefficients of t and t^2 in the exponential expression for the nuclear differential cross section. In the p-p case, in the absence of polarization data, an additional assumption such as spin independence is required to obtain σ_{tot}.

Crudely, the small $|t|$ region (0.001 to 0.1) gives the ratio of Re f(0)/Im f(0) $\equiv \alpha$, the region beyond 0.1 gives b, c and the overall magnitude of the cross section and, by extrapolation, $d\sigma/dt$ (t = 0). The total cross section is then obtained via the optical theorem. Simultaneously with the measurement of $d\sigma/dt$ we intend to measure σ_{tot} by an attenuation measurement and thus provide a check of the procedures and ultimately of the optical theorem. Figure 3 shows a typical $d\sigma/dt$ for

$$\text{Re } f(0) = 0 \text{ and for Re } f(0)/\text{Im } f(0) \equiv \alpha = 0.1.$$

The real parts of f(0) are of interest for two general reasons. First and most fundamentally, they allow (together with σ_{tot}) a test of the forward dispersion relations, at an energy which is an order of magnitude higher than previously available. These considerations apply in πp scattering and also for K-p scattering perhaps with an additional subtraction. Following the analysis of Oehme[1] these measurements would allow a test of microscopic causality down to distances of 10^{-16} cm to 10^{-17} cm.

---

[1] R. Oehme, Phys. Rev. 100, 1503 (1955).

From a more phenomenological point of view, Re f(0) and σ_{tot} are quantities whose energy dependence is predicted by the Regge pole and other theories discussed in the previous section. Among the many possibilities we note two of some interest.

First, the possibility that the Pomeranchuk theorem is violated, i.e. that the leveling out of the Serpukhov cross sections represents an "asymptotic act" predicts that f(0) at high energies become essentially real. Secondly, high energy scattering models with Pomeranchuk generated cuts predict that the asymptotic values of the total cross sections are approached from below. On the basis of this picture one would expect all the total cross sections except $\bar{p}p$ to be rising in the NAL region! Figure 4 illustrates a typical model of this type.

For designing the experiment it is useful to estimate a reasonably pessimistic lower limit to α. We note that if the Serpukhov data are ignored and one uses the fits to the total cross section made by Lindenbaum[2] and assumes the forward dispersion relations, one finds $\alpha \approx 0.03$ to 0.05 at 150 GeV/c and $\alpha \approx 0.05$ to 0.1 at 100 GeV/c. All other calculations known to us give larger values of α. Accordingly, we have set a desired precision in α of $\Delta\alpha = 0.01$.

We turn now to some quasi-experimental considerations. For concreteness we consider πp scattering. We comment that many of the problems encountered have been considered by Foley et al.[3] in their important work on the pion-nucleon forward dispersion relations at AGS energies. Following the notation of Reference 3 we write the differential cross section:

$$\frac{d\sigma^{\pm}}{dt} = \frac{Fc^2}{t^2} \mp \frac{2Fc}{|t|} \operatorname{Im}(A_{N_{\pm}}) [\alpha_{\pm} \cos 2\delta \pm \sin\delta]$$

$$+ (1 + \alpha_{\pm}^2) [\operatorname{Im} A_{N_{\pm}}]^2 \qquad (1)$$

---

[2] S. J. Lindenbaum, "Pion-Nucleon Scattering". Wiley Interscience 1969, edited by G. L. Shaw and D. Y. Wong, p. 111.

[3] K. J. Foley et al., Phys. Rev. Letters 19, 193 (1967).

where $\pm$ refers to $\pi^{\pm}$ p

F_c is the Coulomb amplitude,

$$F_c = \frac{2\sqrt{\pi}\ e^2}{\beta c}\ G_{Ep}\ G_{E\pi}$$

G_{Ep}, $G_{E\pi}$ are the (electric) form factors for the proton and pion respectively.

A_N is the nuclear amplitude.

α = Re A_N/Im A_N and assumed to be constant

$$\delta = \frac{e^2}{\beta c}\ \ell n\ \left(\frac{1.06}{pa\ \theta}\right)$$

p = momentum and a is a "radius" parameter in the Gaussian fit to the form factor.

Figures 5 and 6 show typical values of $d\sigma/dt$ in the interference region. In calculating the figures we have neglected the form factor of the pion and the ct^2 term in the nuclear scattering exponential. Both are qualitatively unimportant.

To investigate the statistics needed for the experiment, we have, by well known techniques, calculated the error matrix we expect to apply after accumulating N events. Again in this calculation we have neglected the ct^2 term which will have only a small effect on the errors in α and σ_T. The result is:

Error Matrix = $\frac{1}{N}$ x

α	b	σ_T	
11.98	16.98	47.02	α
16.98	150.53	215.15	b
47.02	215.15	508.57	σ_T

Thus, to get an rms error in α of 0.01 we need about 120,000 events. Allowing for inelastic triggers we expect to require about 0.5 to 1.0 x 10^6 recorded events per measurement.

As noted in the section on experimental arrangement it is important from a systematic point of view to cover the full t range described so as to avoid problems of relative normalization.

II. C. THE HYPERCHARGE DEPENDENCE OF FORWARD SCATTERING

Our program of studying the elastic scattering of charge particles is particularly relevant to studies of the hypercharge dependence of the strong interactions, within a given family of particles. The possibilities are most striking in baryon-baryon scattering, where we will observe states with four different values of the strangeness:

p-p	$S = 0$
Σ^--p, Λ-p, (Σ^+-p)	$S = -1$
Ξ^--p, Ξ^0-p	$S = -2$
Ω^--p	$S = -3$

In terms of the quark model, we have reactions containing from zero to three strange quarks. These reactions are an ideal testing ground for this model, since the simplest interpretation of present data is that the strange quark has a somewhat different interaction from the non-strange pair.

The least speculative predictions of interactions in the quark model are those dependent on the assumption of additivity of quark amplitudes for forward scattering, since the momentum transfers are then very small. The tests of this model in meson-baryon scattering are well known, and we would look forward to testing these at high energies, where secondary effects are presumably smaller. In baryon-baryon scattering, there are a host of sum rules which may be predicted. A sample of these is given below.[1,2] These are divided into groups, with succeeding groups making the stronger assumptions of spin independence, SU(3) invariance, and high energy limits on quark scattering. Particle labels denote values of the corresponding forward scattering cross sections:

$$\Sigma^+ p - \Sigma^- p = pp - np + \Xi^0 p - \Xi^- p$$

$$\sqrt{3}\,(\Lambda p - \Sigma^0 p) = pp - np - 1/2\,[\Sigma^+ p - \Sigma^- p]$$

---

[1] D. A. Akyeampong, Nuovo Cimento 48A, 519 (1967).

[2] Dare, Nuovo Cimento 52A, 1015 (1967).

$$\Lambda p = 1/2\ [\Sigma^+ p + \Sigma^- p]$$

$$pp + \Lambda p = np + \Sigma^+ p$$

$$\Sigma^- p = \Xi^o p$$

$$\Sigma^+ p = np$$

$$np = 1/2\ [\Lambda p + pp]$$

$$\Lambda p + \Xi^- p - 2\ \Sigma^- p = 3/4\ [np - \Sigma^+ p]$$

$$3\ [2\ \Lambda p - \Sigma^- p] = 4\ np - \Sigma^+ p$$

$$np = pp,\ \Lambda p = \Sigma^- p = \Sigma^+ p$$

$$\Xi^- p = \Xi^o p$$

$$\Lambda p = 1/2\ [np + \Xi^o p]$$

Aside from the quark model, one can test the predictions of SU3 for the baryon-baryon scattering amplitudes. This is again a favorable place for a test because of small momentum transfers. One needs at least three hyperon cross sections, in addition to the nucleon cross sections, to carry out a test. This should be possible in our experiment, since we should obtain the $\Sigma^- p$, $\Xi^- p$, and Λp cross sections.

III. A. HIGH RESOLUTION DETECTORS

This experiment relies on the use of novel detectors with high spatial resolution. Since these are described only in as yet unpublished reports, a summary of the work which has been done and the characteristics of these detectors may be of interest here. Members of the team presenting this proposal have worked on high resolution spark chambers[1,2] and high resolution proportional chambers[3]. At the present moment, the wire spark chambers have higher accuracy, and our experimental design is based on the resolution which can be achieved in this way with the techniques we have demonstrated. This resolution, 50 μm, is about five to ten times better than that usually achieved in wire spark chambers.

A parallel effort in proportional chambers is yielding very encouraging results. We are confident of achieving an effective resolution within a factor of three of the above value with the present techniques, and we may reasonably hope for further improvements in the near future. Our plan for this experiment is to prepare the wire spark chambers which we know will provide the resolution needed, but to pursue the proportional chamber development as well. If the latter turn out to meet the resolution requirement, we would certainly adopt them to gain the advantage of a factor of a hundred or more in rate and much better time resolution.

The improvement in the performance of the wire spark chamber resolution derives from a program which attacks each of the primary limitations in wire spark chamber accuracy. The diffusion of electrons in the spark

---

[1] W. J. Willis, W. Bergmann, and R. Majker, "High Resolution Optical Spark Chambers," (to be submitted to Nuclear Instruments and Methods).

[2] W. J. Willis and I. J. Winters, "High Resolution Wire Spark Chambers," (ibid.).

[3] M. Atac and J. Lach, "High Spatial Resolution Proportional Chambers," NAL Report FN-208, April 1970.

chamber gas, the basic limitation, is reduced by increasing the gas pressure. The effect of structure and instabilities of the spark column is reduced by reducing the gap width, and thus the spark length. This is permissible because of the higher pressure, which increases the number of ions per unit length, and reduces the spark formation time. Reducing the gap width also decreases the effects of track inclination to the spark chamber plane. In using magnetostrictive readout, the resolution is improved by reducing the size of magnetostrictive wire in the pick-up coil, and by providing a scale magnification by fanning out the wires to four times larger spacing at the readout line.

The wire planes which have been used so far are etched from 10 μm copper on a Kapton backing, with a spacing of eight wires per millimeter. A spacing of twelve wires per millimeter is also feasible with the same technique. The chamber is operated at a pressure of 5-15 atmospheres of 90% neon, 10% helium, 1% argon, 0.1% CH_4. A set of these chambers 4×4 cm^2 has been operated in a low energy test beam to measure the resolution. The results, which were limited by multiple scattering, gave an upper limit on the resolution of 65 μm (1 standard deviation limit). It should be possible to attain 25 μm resolution with these chambers. In gases at reasonable pressures, diffusion sets the ultimate resolution limit at 10-15 μm.

The developments in proportional chambers have so far relied on careful field shaping and the possibility of variable pressure[3]. Chambers have been operated with a spacing of one and two wires per millimeter. Both chambers operate well, and the former has been operated in a test beam, with demonstrated efficiency and resolution. With a pair of staggered chambers, this promises 125 μm resolution. Further development is continuing steadily, and within a few months we should know if it is possible to produce proportional chambers of the required resolution at the date needed for this experiment.

III. B. ANGULAR AND MOMENTUM RESOLUTION REQUIREMENTS

We wish to measure elastic scattering at energies up to 200 GeV, with an accuracy in momentum transfer which allows the measurement of the angular range in which Coulomb single scattering is dominant, in an experiment which covers the diffraction peak. In a 0.5 m hydrogen target, this is the transverse momentum range from ~30 MeV/c to ~60 MeV/c. Smaller transverse momenta are dominated by plural scattering, larger by nuclear scattering (see Fig. 3).

One potential limitation is the multiple scattering in the pair of detectors on the upstream and downstream ends of the hydrogen target. Each unit will contain three x-y spark planes, or a total of six, together with the neon gas and chamber windows. The average transverse momentum due to multiple scattering imparted by the whole assembly is 3.0 to 4.0 MeV/c, depending on design details affecting the length of gas, etc. This turns out to be the same as the multiple scattering in the hydrogen target of ~1/2 meter length, and is much smaller than the lower end of the range of transverse momenta in scattering in the range to be measured. The plural scattering in the detector is important up to ~25 MeV/c, but most of this will be removed in the analysis since the space resolution of the chambers is sufficient to distinguish whether the origin of scatters of more than 15 MeV/c is in the detector or in the target. In short, the scattering in the detector does not limit this aspect of the experiment.

The lever arm needed to equal the error due to scattering is calculated assuming two pairs of detectors on either side of the target, each separated by length L. Each detector is assumed to provide two measurements of each coordinate, with resolutions of 50 μm. The error in scattering angle is then $\sqrt{2} \times 50\ \mu m/L$, and the corresponding transverse momentum for a particle of momentum 200 GeV/c is

$$P_\perp = 2 \times 10^5 \times \sqrt{2} \times 50 \times 10^{-6}/L$$
$$= 14\ \text{MeV/c/L}$$

The length needed to give $P_\perp = 3.5$ MeV/c is 4 m.

The momentum of the incoming particle is measured from the properties of the beam and its position at the appropriate location. The momentum of the outgoing particle is measured by the decay spectrometer, in the case of the short lived particles, and by deflection in a bending magnet in the case of the long lived particles. In the latter case, the multiple scattering is the limitation of the accuracy:

$$\frac{\Delta p}{p} = \frac{P_\perp \text{ due to multiple scattering}}{P_\perp \text{ due to bending magnet}}$$

We propose to use two standard 20 foot NAL main ring magnets at 20 kG, which gives $P_\perp$ = 7200 MeV/c, and thus $\Delta p/p$ = 0.05%. The highest momentum particles from inelastic processes differ from elastically scattered particles by 0.07% at 200 GeV/c.

III. C. LONG LIVED PARTICLE EXPERIMENTAL ARRANGEMENT

The short lived particles can be identified by their decays, thereby easing the problem of the mass identifying Cerenkov counter. The identification of the more stable particles must rely on the operation of refined Cerenkov counters. For this and other reasons it is desirable to perform this part of the experiment in the high resolution 2.5 mr beam. The layout is shown in Fig. 7.

The angle of the particle is measured before and after the 1/2 meter hydrogen target by small high resolution detectors. The momentum of the scattered particle is measured by the deflection in two accelerator magnets. The lever arms are set by the considerations discussed in the section on Angle and Momentum Resolution, taking into account the experimental details. For example, the lever arm after the magnet is made larger because the final chamber is somewhat larger, about 10 cm, than those near the target, and may not display the same accuracy we have achieved in our 4 cm chambers.

The excess drift space near the target is provided so that we can distinguish scatters in the hydrogen target from those in the adjacent detectors, and thereby eliminate that source of background from the final data. Our resolution implies an accuracy of < 0.7 m in the longitudinal position of the scattering at the smallest scattering we would contemplate analyzing, a transverse momentum of 15 MeV/c.

The trigger is defined by suitable Cerenkov signals, location of the particle at the dispersive focus of the beam, the defining counters immediately preceding the first spark chamber, S_1, and no count in the 2 mm veto counter between the two magnets. The incident beam, with a focal spot $\sim$0.9 mm in diameter[1], is focused on this counter. The dispersion due to the preceding magnet, for $\Delta p/p = 1\%$ is 0.7 mm. If it is necessary to

---

[1] D. Reeder and J. MacLachlan, 1969 Summer Study, NAL, Vol. 1, p. 41.

decrease the solid angle or momentum bite of the beam, to maintain the ideal focal spot diameter, the larger solid angle of our apparatus allows this to be done with little or no sacrifice in data rate.

The hydrogen target is surrounded by a proton detector. Although the detection of the proton is not required, its observation will be used as a check, in those events in which it has enough momentum to escape the target.

The transverse momentum range accepted through the apparatus is just under 1 GeV/c for 200 GeV/c incident or 250 MeV/c for 50 GeV/c incident. This means that over the whole region of interest one can observe a large portion of the diffraction peak without disturbing any of the equipment. We believe that this is very important in avoiding systematic errors in the Coulomb interference and diffraction peak shrinkage experiments. To cover this range of $|t|$ with conventional detectors would require a very large investment in magnets.

III. D. HYPERON EXPERIMENTAL ARRANGEMENT

General

This phase of the program breaks naturally into two parts. The first is a survey of hyperon production and search for new particles, and the second is a study of the small angle hyperon-proton scattering. Here, we intend to study the range of t from $|t| \cong 0.1$ to $|t| \cong 0.6$ for which one may usefully detect the recoil proton. Detection of the recoil is necessary in the hyperon scattering experiments in order to provide a trigger which efficiently selects scattering events.

Figure 8 is a diagram of the experimental arrangement of the short lived particle phase of the program. A beam of 200 GeV protons impinges on a target of cross section 1 mm x 1 mm and approximately one interaction length in the beam direction. High energy negative particles produced in the forward direction are transmitted by a magnetic channel. Following the channel approximately 5 m is available to insert precision wire chambers, focusing Cerenkov counter, and/or a liquid hydrogen target. A focusing Cerenkov counter will be used in the new particle search and as a check in the survey of hyperon production fluxes. Then begins the decay region followed by the first analyzing magnet, A1. This magnet allows a determination of the momentum of the low energy particles, leptons, and mesons, produced in the decay. The high momentum protons produced through a decay chain such as

$$\Omega^- \rightarrow K^- \Lambda^0$$
$$\hookrightarrow \pi^- p$$

are further deflected from the long lived component of the negative beam by A2. They strike the proton trigger counter shown in Fig. 8. High energy neutrons produced in decays such as

$$\Sigma^- \rightarrow n \pi^-$$

are identified in the neutron shower counter indicated in the same figure. We now discuss the arrangement in more detail.

The Magnetic Channel

The magnetic channel we have chosen is 6 m long and is a modified main ring bending magnet. Figure 9 is a cross section view of this magnet. The inner coils of a standard main ring magnet have been removed and the pole tips closed down to a gap of 1 cm. Computations with the LRL magnet design code, LINDA, indicate that with this modified configuration one could achieve a field of 40 kG. The channel is tapered in the horizontal plane from an aperture of 2 mm increasing to 6 mm at the channel exit. The channel has as its central momentum 150 GeV/c at a field of 30 kG. With this channel geometry one could easily deflect particles of up to the full beam energy down the channel. The actual design would have an enlarged portion of the channel in the region of the target so as not to confuse interactions in the walls with those in the target. The properties of this channel have been investigated extensively using a Monte Carlo computer code. The full momentum band transmitted by the channel is 10%. However, momentum and exit position and angle are high correlated, and with our detectors the momenta of individual hyperons can be determined to within 0.1%.

Hyperon Fluxes

We have used the hyperon production cross sections suggested by Sandweiss and Overseth[1] to estimate the hyperon fluxes emerging from our magnetic channel and surviving to 5 m beyond it which is the start of the

---

[1] J. Sandweiss and O. Overseth, TM-199, NAL, January 1970.

decay region. They estimate that using 200 GeV incident protons to produce Σ^- at 150 GeV/c in the forward direction the cross section is

$$\frac{d^2N}{d\Omega dp} = 0.038\ \Sigma^-/\text{int. proton/ster/GeV/c.}$$

For the channel we have described and for 10^{10} protons interacting in our target this results in a flux of

$$1775\ \Sigma^- \text{ per pulse.}$$

If we assume the production cross section for Ξ^- is lower by a factor of 30 and of Ω^- by a factor of $(30)^2$ we observe at 150 GeV/c

$$60\ \Xi^- \text{ per pulse}$$
$$0.6\ \Omega^- \text{ per pulse.}$$

Using the Hagedorn-Ranft computations[2] we will also have emerging from our channel

$$83{,}000\ \pi^- \text{ per pulse.}$$

This is a flux of pions which will give no problem with accidentals and indicates that incident proton fluxes of up to 10^{11} protons per pulse might be desirable.

An estimate of the Σ^+ has been made by Hagedorn-Ranft[2] and give at 150 GeV/c for 10^{10} interacting protons per pulse

$$35{,}000\ \Sigma^+ \text{ per pulse.}$$

The proton and π^+ contribution to the beam will be according to the same Hagedorn-Ranft computation

$$3{,}000{,}000 \text{ protons per pulse}$$

and

$$450{,}000\ \pi^+ \text{ per pulse.}$$

---

[2] T. G. Walker, NAL, 1968 Summer Study, Vol. 2, p. 59.

If these predictions have any validity we should be able to extract a fair amount of physics with this Σ^+ beam. There are no predictions for the expected yields of the other positive hyperons.

High Resolution Cerenkov Detector

A high resolution Cerenkov counter[3] used at the magnetic channel exit would provide detection of hyperon fluxes regardless of their decay mode. This counter would be used to check the production fluxes at the known hyperons, which would be determined primarily by decay identification, and to search systematically for new particles which might not be detectable via their decay with our apparatus. The results of our studies can now be summarized as follows:

1) We propose the construction of a 4-meter, low-pressure gas focusing Cerenkov counter. The cone angle will be from 7 to 12 mrad, a parabolic or spherical mirror will be used, and a ring aperture on a single 2-inch fused silica-window photomultiplier will provide velocity selection and hence particle identification. The attainable resolution in β, limited by the energy spread of the beam and the angular divergence accepted, will be in the range 5 to 10 x 10^{-6}, and will be adjusted to just separate adjacent mass particles; the most severe requirement is the Σ^--Ξ^- separation. The data of Reference 4 indicate that we should average 8 photoelectrons per particle.

2) Suitable angular restriction of the accepted beam, which must be held to ±0.2-0.3 mrad, will be obtained from coincidences with the hodoscopes required to determine the hyperon direction with high precision.

---

[3] A. Roberts, M. Atac, R. Stefanski, NAL internal report

[4] Yu. P. Gorin et al., IHEP 69-63, Serpukhov 3-20 (1969).

3) The dispersion and momentum acceptance of the presently conceived magnetic channel are such that the angular restriction required for the Cerenkov counter will admit only about 1-2% of the total hyperon beam. This appears to be adequate for survey purposes, although not for experiments on the rarer hyperons.

4) The resolution of the counter is adequate for separation of all particles heavier than kaons; it is marginal for kaon-pion separation and inadequate for lighter particles. For survey purposes, the resolution can be varied, so that it is adjusted to be sufficient for the known hyperons; for a search for heavier particles, it can be decreased to make the search easier. The mass search is conducted by varying the counter pressure, thus varying the velocity interval accepted.

Hyperon Decay Spectrometer

Table 1 is a summary of the maximum decay angles of the hyperon decays of interest at 150 GeV/c. For comparison we also list the decay angles at 23 GeV/c which are appropriate to the hyperon experiment being done by this same group at Brookhaven National Laboratory. The angles of the two experiments scale approximately as the ratio of the momentum of the hyperons. The most crucial measurement is the determination of the hyperon angle which is accomplished by high resolution wire chambers. As was mentioned earlier we believe we can achieve spatial resolutions of 50 μ which means that the initial hyperon direction can easily be determined to the required accuracy before and after scattering from the 40 cm liquid hydrogen target in the 5 m between the magnetic channel and the start of the decay region. For both the initial hyperon flux measurements and the hyperon scattering experiment the hyperons will be identified by their decay products. It is worthwhile to consider in some detail the kinematics of the relevant decays. Consider first the decay of $\Sigma^- \rightarrow n\pi^-$. The π^- angle and momenta are determined by spectrometer A1 and wire spark planes of conventional design (resolution $\sim$0.3 mm). The neutron direction is determined

by a hadron shower counter similar to the one used in our BNL experiment. To achieve equivalent angular resolution, assuming the neutron interaction position can be determined to about 1 cm requires a neutron detector of 1 m x 1 m in size positioned about 100 m from the channel exit. The neutrons resulting from the Σ^- decay are of high energy and the neutron detector need only give us a very crude indication of energy.

The signature of the Ξ^- will be

$$\Xi^- \rightarrow \pi^- \Lambda^0$$
$$\qquad\quad \hookrightarrow \pi^- p .$$

The π^- kinematics are determined by A1 as well as the properties of the π^- resulting from the Λ^0 decay. The proton from the Λ^0 decay is further deflected by A2 and is well separated ($\sim$0.75 m) from the π^- beam emerging from the channel at about 50 m from it. Here a wire chamber array and a proton trigger counter will be located. The emergence of a positive nucleon from a well defined negative beam should provide a powerful trigger for Λ^0 events. The kinematics and triggering of the $\Omega^- \rightarrow K^- \Lambda^0$ decays is qualitatively similar but can easily be distinguished in this highly overconstrained fit (4c) from the Ξ^- decay. The apertures required of A1 and A2 are modest. Standard BNL 18D72 magnets would be adequate.

We note that the hyperon beam described here offers many potential advantages for the study of rare hyperon decay modes. In particular the longer decay lengths at NAL energies implies substantial improvements both in absolute rates and in beam background. We anticipate that the production fluxes and the developing techniques of particle identification at high energies will make these experiments feasible and attractive.

New Particle Search

The beam geometry used for the short-lived particle phase of this experiment is ideal for a search for new particles of lifetime 10^{-11}-10^{-10} seconds. This lifetime range is not accessible to the conventional beam

survey experiments. Such particles are detectable with a focusing Cerenkov counter or by their decay products. The detection via the Cerenkov counter would, of course, be independent of decay mode; but because of the limited angular acceptance of the Cerenkov counter only about 1-2% of the beam could be counted. The flux of such a presumed particle would depend on three factors; its production cross section, its lifetime, and mass. Figure 10 indicates the regions of these variables in which our search would be significant. In that figure we relate the production cross section of our particle to that of the Hagedorn-Ranft π^- production cross section. We have plotted for a given production cross section the lifetime versus mass which would give us one count in the Cerenkov detector for 10^{11} interacting protons. The efficiency of the Cerenkov counter (1%) has been included in these calculations. Both positive and negative particles could be investigated in this manner.

For the case of detection via decay only, the sensitivity would be increased by a factor of 50-100 (the loss due to Cerenkov acceptance) but reduced by its branching ratio into a detectable decay mode.

In the decay experiment the system trigger would be various combinations of a high momentum neutral or positive particle (presumably the fast baryon) in coincidence with a lower momentum particle (presumably meson or lepton).

V. SUMMARY OF RATES AND BEAM REQUIREMENTS

Coulomb Interference Measurements with Stable Particles

In this case data taking will be limited by the dead time of the apparatus. This is easily seen given that the effective cross section is $\approx$1-2 mb for elastic events or about one event every 300 to 600 beam particles. Typical π fluxes available are $\approx 10^5$ per pulse and K fluxes are 10^3 to 10^4 per pulse. Furthermore, we have assumed that only about 1/8 of all triggers are true elastics. Thus assuming a 1 sec spill and a 10 ms spark chamber dead time we expect about 12 elastics per pulse.

As argued previously, about 10^5 elastics are needed for each measurement point (i.e., particle and momentum) to give an error in α = Re f(0)/Im f(0) of 0.01. This amounts to about 10 hours per measurement.

We would propose a measurement matrix of π^+, π^-, K^+, K^- p and $\bar{p}$ each at three energies, giving a total of 180 (ideal) hours for this phase of the experiment. Obviously, if the precision proportional chamber development is successful the time required will be less by an order of magnitude.

Diffraction Peak Measurements with Hyperons

Here, at least for the Ξ^- and Ω^-, the experiment is limited by available beam flux. On the other hand we do not attempt to measure the Coulomb interference so less data is needed. As noted earlier in these measurements we must detect the recoil proton and measure its energy. This limits the t range to $|t|$ = 0.1 to 0.6. Also measurements will most likely not be made for the anti-hyperons so the measurement matrix is smaller than for the stable particles. These factors nearly compensate and we expect that this phase of the experiment will also take about 200 hours of ideal time to complete. It should be noted however that there are large uncertainties in the estimates of the hyperon fluxes, particularly for the Ξ^- and Ω^-. These fluxes will hopefully be better estimated after the BNL Y^- experiment has run in 1970-71.

Experimental Equipment Required

Much of the counting and data collecting equipment required for the experiment is very similar to that being developed by this group for the BNL hyperon experiment. Both the hyperon phase and the long lived particle elastic scattering phase will require an on-line data collecting computer such as the NAL PDP-15 which will be used for the BNL hyperon experiment. The interfaces being developed for its BNL usage would also be needed for this experiment, and it is requested that this same machine be made available to us. Ideally, as in our BNL usage, we would like a link from the PDP-15 to a larger machine capable of carrying some fraction of the data through to the final analysis. However if this is not available access to a larger on-site computer which would be capable of reading the magnetic tape output of the PDP-15 would be essential.

The hyperon phase of the experiment will require a high energy (~200 GeV) proton beam of intensity 10^{10}-10^{11} protons per pulse focused to a spot of about 1 mm in cross sectional area. We believe the proposed diffracted proton beam planned for Area 2 would be suitable. We believe the magnetic channel can be a main ring bending magnet with the inner coils removed and magnet channel sketched in Fig. 9 inserted. Two analysis magnets comparable to BNL 18D72 magnets and a liquid hydrogen target complete the list of requirements of the hyperon phase.

The long lived particle phase requires a beam of good momentum resolution and most importantly of optical quality such that Cerenkov counters capable of distinguishing π, K, and p from each other could be incorporated into it. It must be capable of a focal spot of about 1 mm in diameter. Two NAL main ring magnets are used for the momentum analysis of the scattered particles.

Table 1

Hyperon Decay Kinematics

Maximum Laboratory Angles

		23 GeV/c	150 GeV/c
$\Sigma^- \rightarrow n\pi^-$	θ_n	10.7 mr	1.63 mr
	θ_π	71.7	11.00
$\Xi^- \rightarrow \Lambda^o\pi^-$	θ_{Λ^o}	7.15	1.10
	θ_π	57.2	8.78
$\Omega^- \rightarrow \Lambda^o K^-$	θ_{Λ^o}	19.1	2.93
	θ_K	153.0	23.4
$\Lambda^o \rightarrow \pi^- p$	θ_p	5.17	0.79
	θ_π	34.8	5.34

Figure 1

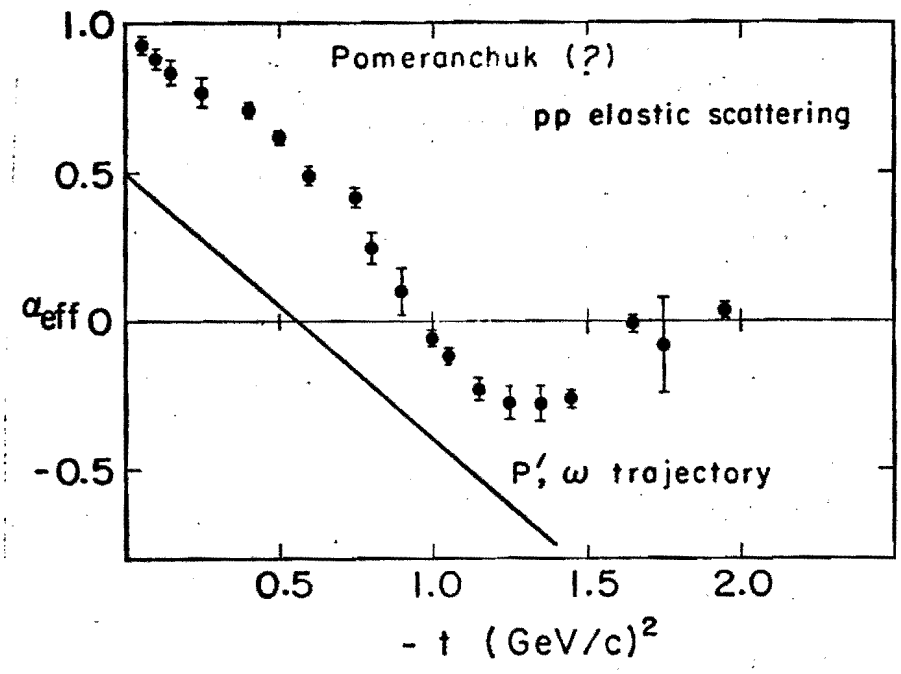

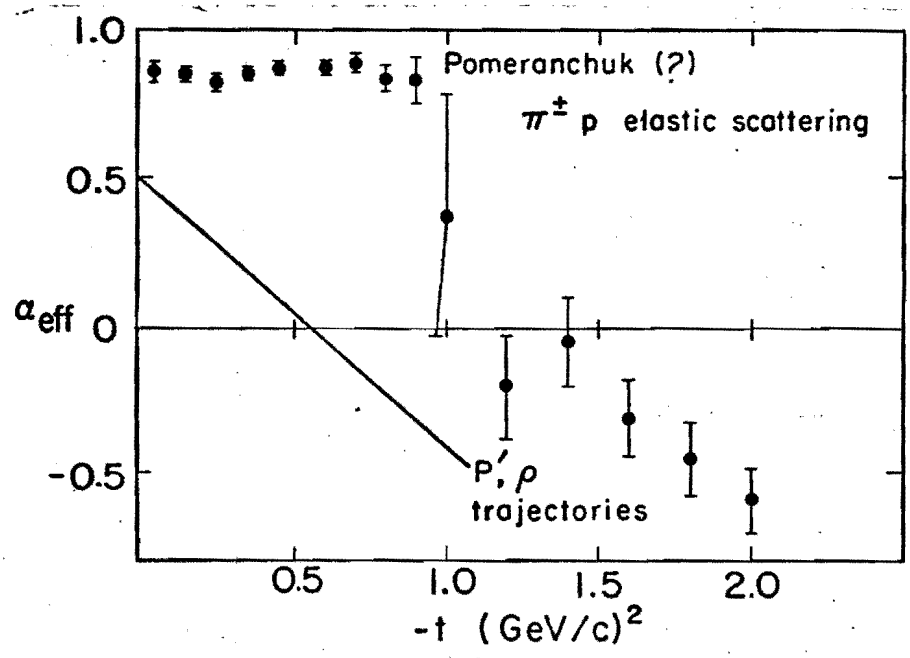

From; G. Fox, High Energy Collisions

Figure 2

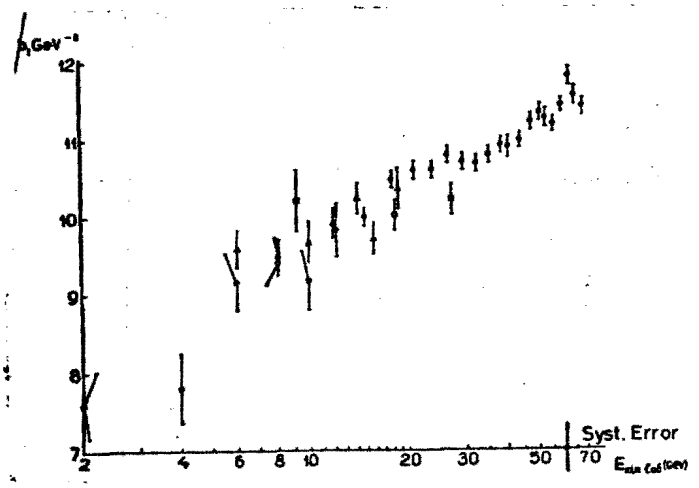

The slope parameter b, from elastic proton-proton collisions (see text) as a function of energy. The symbols represent data from Ref. 14, Ref. 16, Ref. 17 and Ref. 18.

$\pi^+ p$ at 100 BeV/c

Figure 3

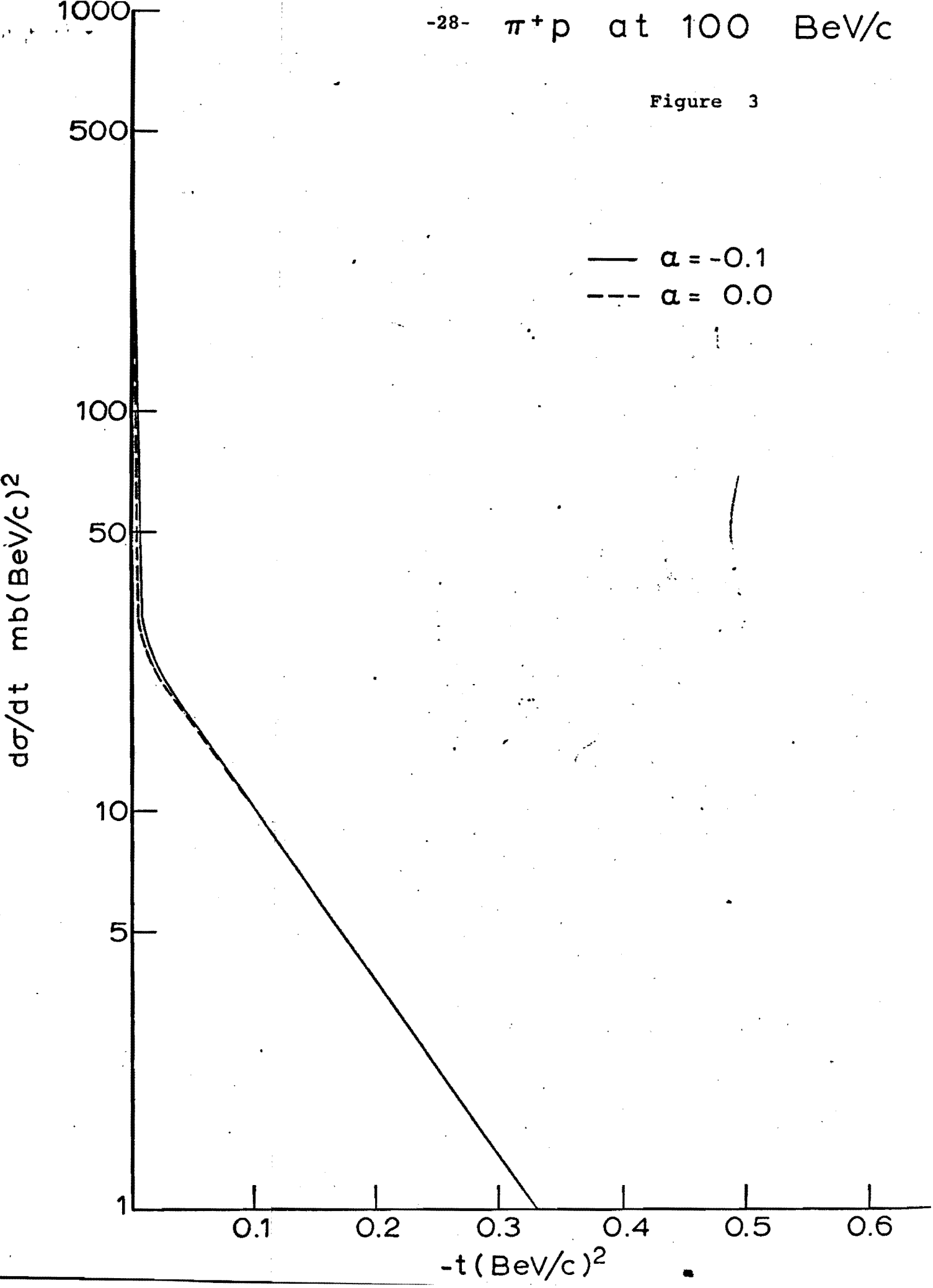

Figure 4

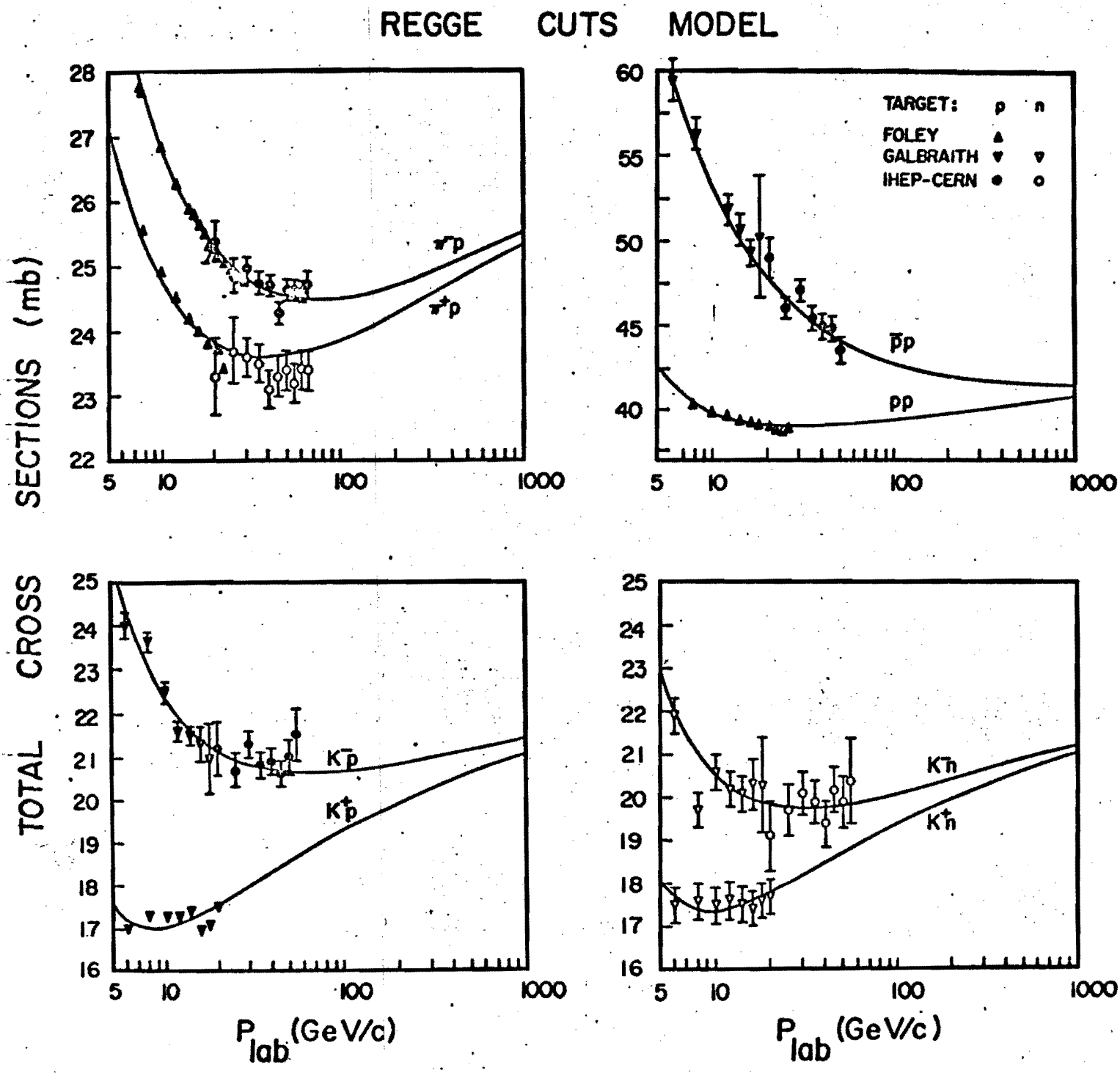
REGGE CUTS MODEL
TOTAL CROSS SECTIONS (mb)
$\pi^- p$
$\pi^+ p$
$\bar{p}p$
pp
TARGET: p n
FOLEY
GALBRAITH
IHEP-CERN
$K^- p$
$K^+ p$
$K^- n$
$K^+ n$
P_{lab} (GeV/c)
P_{lab} (GeV/c)

Figure 5

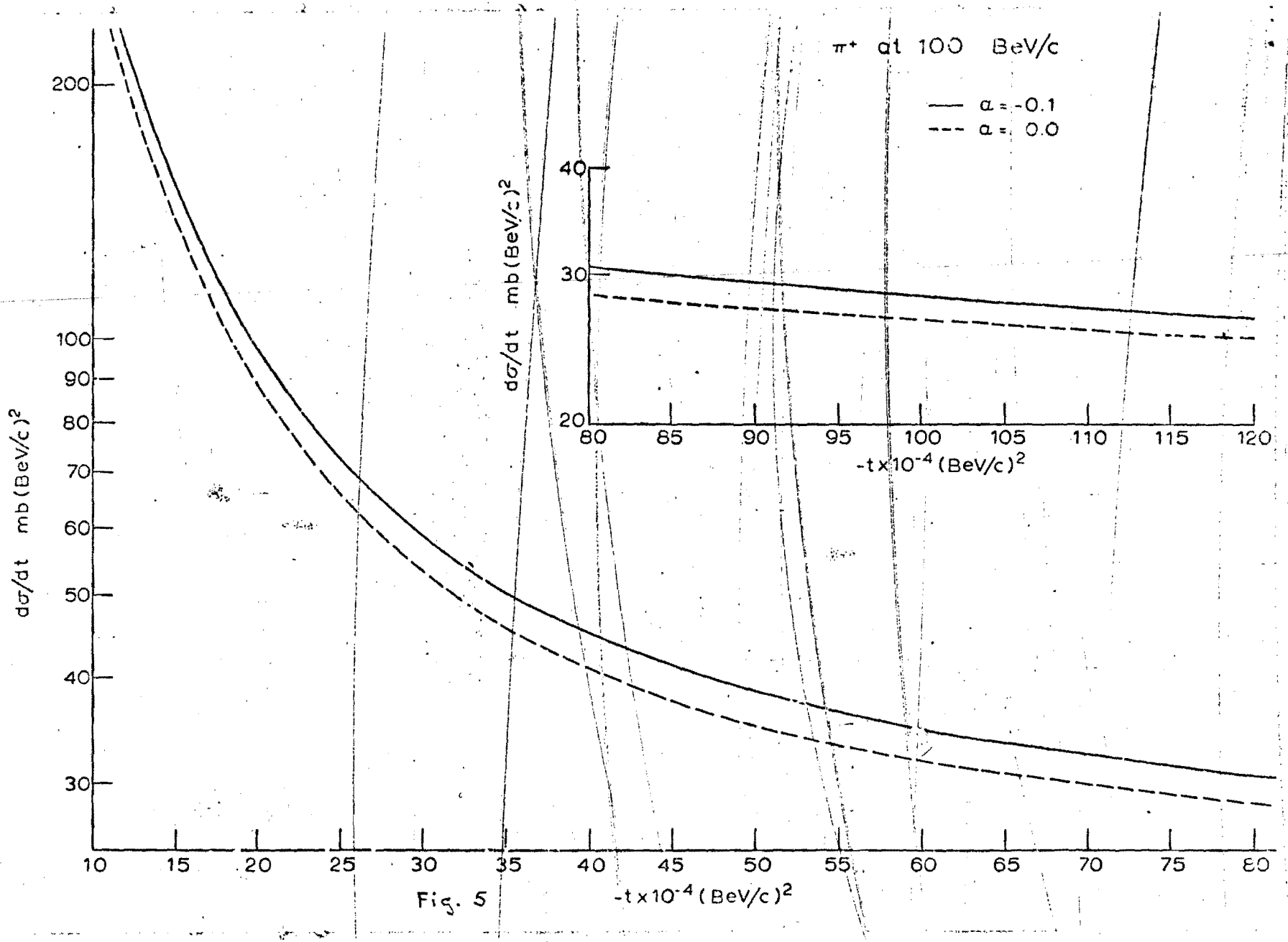

Fig. 5

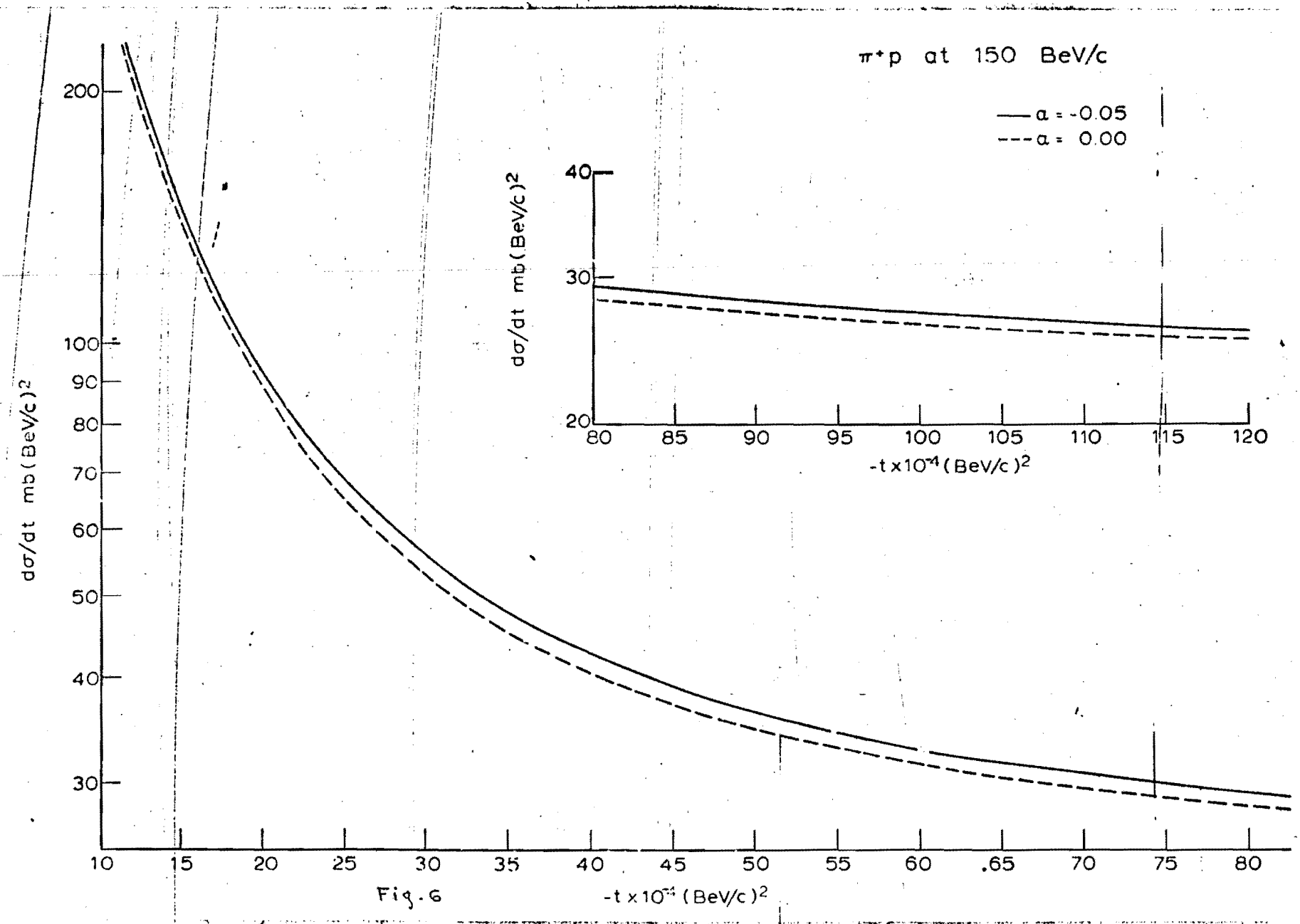
π⁺p at 150 BeV/c
— α = -0.05
--- α = 0.00
dσ/dt mb(BeV/c)²
-t x10⁻⁴ (BeV/c)²
200
100
90
80
70
60
50
40
30
10
15
20
25
30
35
40
45
50
55
60
65
70
75
80
40
30
20
80
85
90
95
100
105
110
115
120

Fig. 6

Figure 7

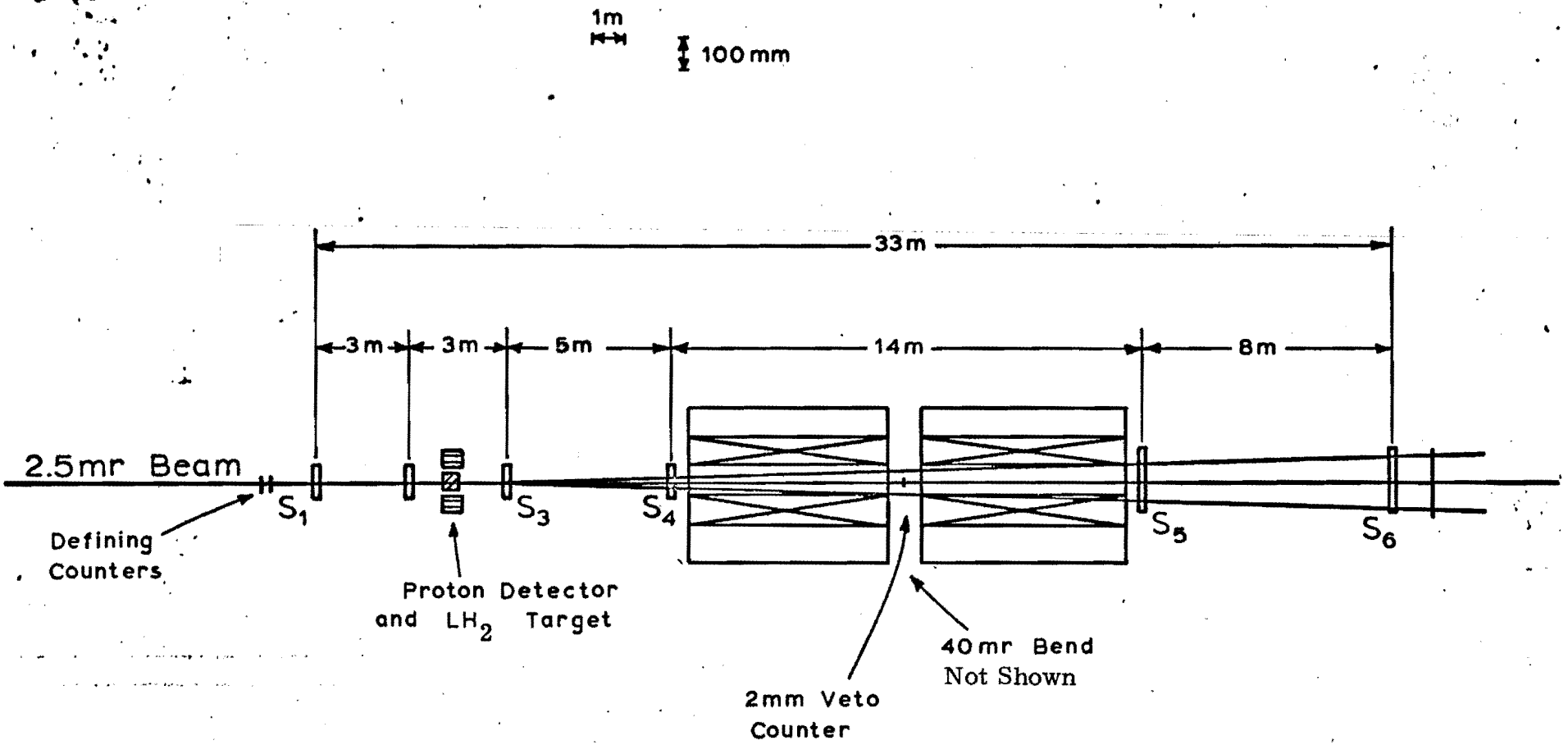
1m
100mm
33m
3m
3m
5m
14m
8m
2.5mr Beam
S_1
S_3
S_4
S_5
S_6
Defining Counters
Proton Detector and LH_2 Target
2mm Veto Counter
40mr Bend Not Shown

Figure 8

Hyperon Experimental Arrangement

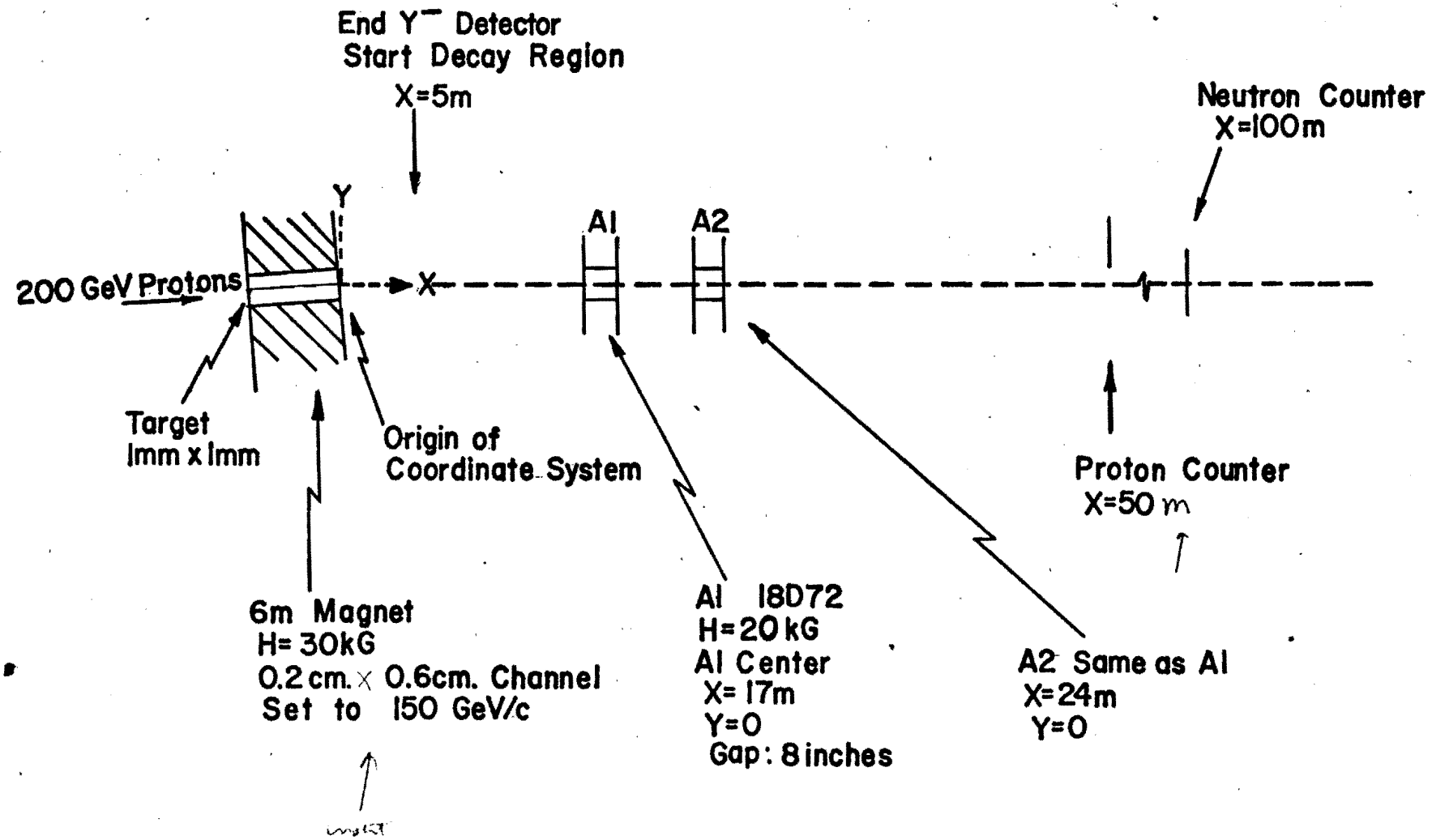

Figure 9

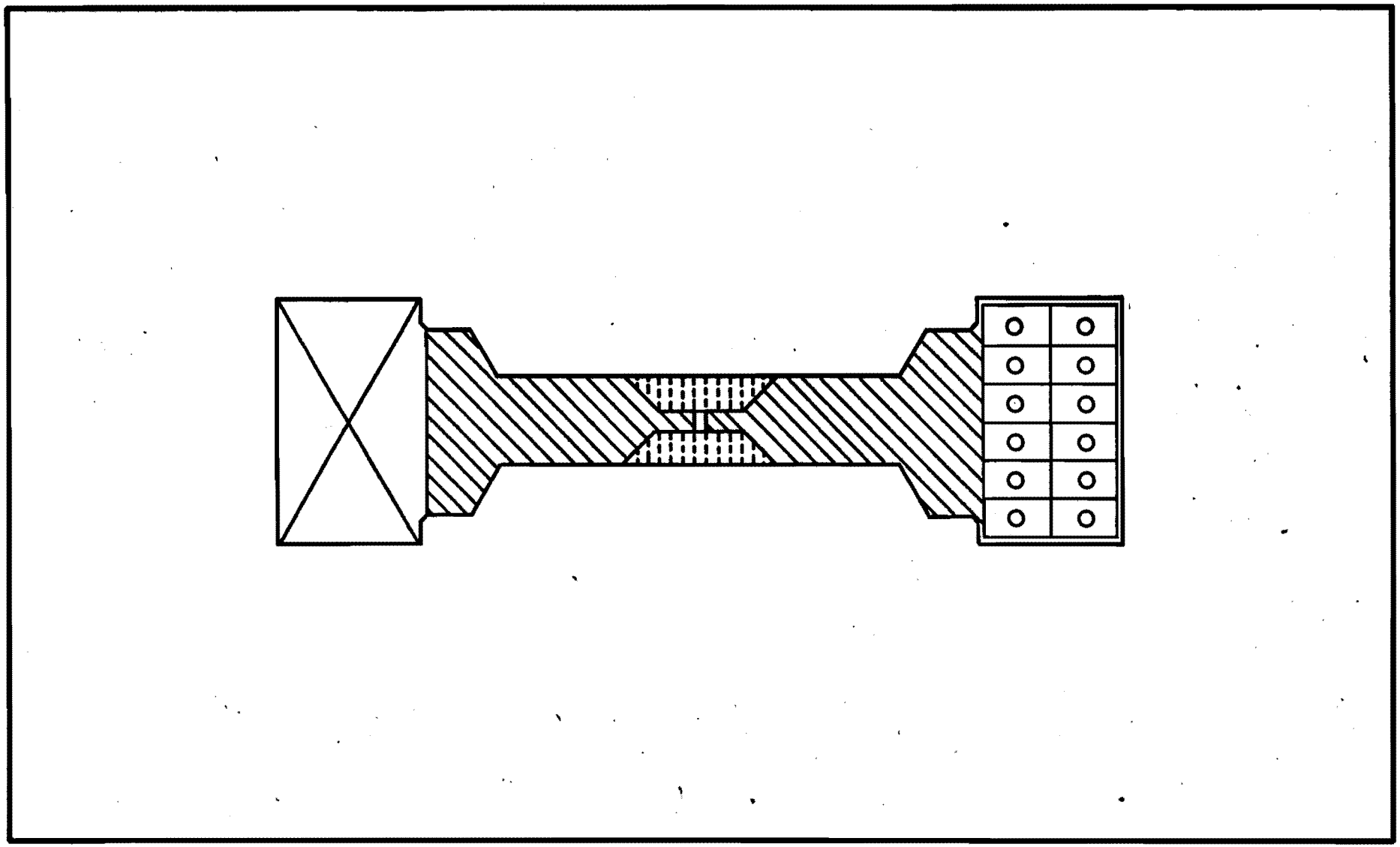

Scale: 2.5" per inch

Brass Shield

Co-Fe Pole Tip

Figure 10

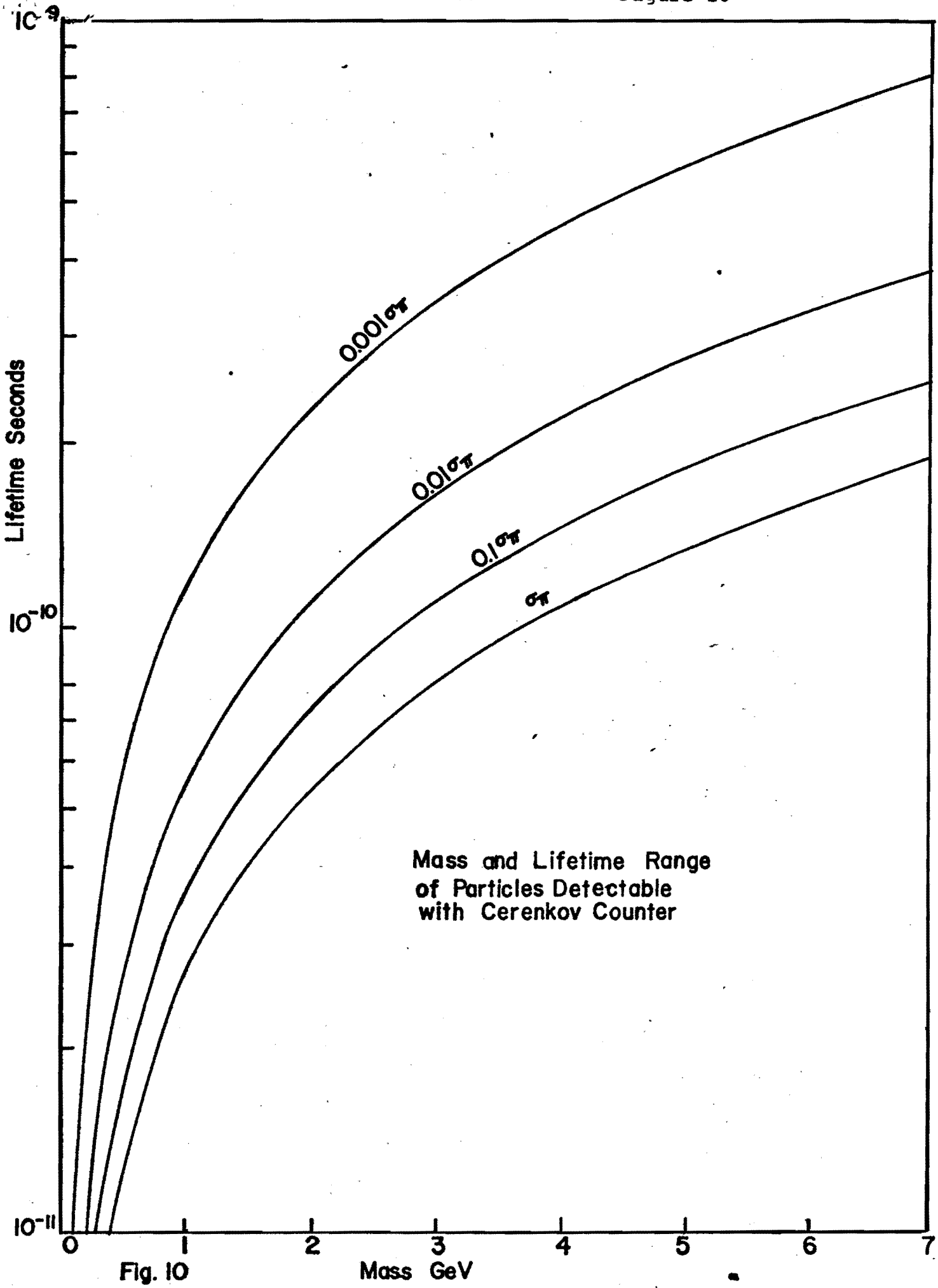

Fig. 10

REVISED

NAL PROPOSAL NO. 69

Correspondent: W. J. Willis
Sloane Physics Laboratory
Yale Univesity
New Haven, Connecticut
FTS/Commercial 8-203-436-1580 06520

ELASTIC SCATTERING OF THE LONG-LIVED HADRONS

M. Atac, C. Dolnick, P. Gollon, J. Lach,
J. MacLachlan, A. Roberts, R. Stefanski, D. Theriot

National Accelerator Laboratory

H. Kraybill, J. Marx, P. Nemethy, J. Sandweiss
W. Willis

Yale University

December 1, 1970

May 1971, New Scientific Spokesman

ELASTIC SCATTERING OF THE LONG-LIVED HADRONS

We propose to measure the elastic scattering of the charged hadrons $\pi^{\pm}$, $K^{\pm}$, p and $\bar{p}$ over a region of momentum transfer up to about 1 GeV/c. Special attention will be given to the Coulomb interference region. This experimental program is based on the use of novel detectors of high spatial resolution which we have developed.

M. Atac, C. Dolnick, P. Gollon, J. Lach, J. MacLachlan
A. Roberts, R. Stefanski, and D. Theriot
National Accelerator Laboratory

H. Kraybill, J. Marx, P. Nemethy, J. Sandweiss,
and W. Willis
Yale University

December 1, 1970*

Correspondent: J. Lach

*This and Proposal 97 were originally submitted together as one proposal on June 15, 1970.

I. INTRODUCTION

We propose to measure the small angle scattering of esentially all the stable charged particles. For some time we have been developing detectors of high spatial resolution - almost an order of magnitude greater than that obtained in normal wire spark chambers - necessary to do experiments with beams of high energy hyperons. While these detectors are essential for these experiments, because of the short lifetime of the hyperons, they offer tremendous advantages of convenience and economy when applied to the small angle scattering of the stable particles. For an experiment with a fixed momentum transfer acceptance, the weight of analyzing magnets can be reduced by one to two orders of magnitude, with a corresponding decrease in the space occupied by the apparatus.

These technical developments coincide well with our interest in the physics of small angle scattering: the change in shape or "shrinkage" as energy is increased; the measurement of the forward scattering amplitudes and comparison with SU 3; the measurements of the real part of the forward scattering amplitude and thus the measurement of the total cross section by the optical theorem in a very clean way; and, especially, the application of these results to tests of the forward dispersion relations and the validity of relativistic quantum mechanics.

II. A. ENERGY DEPENDENCE OF SMALL ANGLE SCATTERING

In the last ten years this has been one of the topics in particle physics most discussed by theorists. Here we risk oversimplifying the issues to bring out what seems to be the most crucial question to be settled by going to high energy. This is whether the scattering of small momentum transfers approaches an energy dependent form as the energy increases, or continues to exhibit a steady shrinkage.

The different theories developed to explain elastic scattering divide rather clearly on this point. Theories of the Regge-pole type with a Pomeranchuk trajectory roughly parallel to other known trajectories predict a shrinking of the diffraction peak for all scattering processes, that is, a continuous increase of slope of the $d\sigma/dt$ as a function of energy. On the other hand, theories with a fixed Pomeranchuk singularity, that is a trajectory showing a very small slope increase with momentum transfer, as well as a wide class of theories related to the optical model such as that of Chou and Yang[1] or Durand and Lipes[2], predict an asymptotic approach to an elastic scattering differential cross section which is independent of energy, particularly at small $|t|$.

What we now know is that at AGS energies, some peaks shrink (p-p), some grow ($\bar{p}$-p), and some remain constant (π-p). Figure 1 illustrates this situation. The fashion among Regge theorists recently has been for a flat Pomeranchuk trajectory. The observed variations with energy are then

ascribed to secondary trajectories, while effects at large $|t|$ are obscured by cuts. Thus the question can only be resolved by experiments at higher energy and at very small $|t|$. Great interest has been aroused by the only higher energy result available, the p-p scattering from Serpukhov. There it seems that the p-p elastic peak does not stop shrinking, but rather indicates a Pomeranchuk trajectory with a large slope, Figure 2. If these results are really correct, perhaps we will find that at sufficiently high energies the π-p and $\bar{p}$-p peaks will begin to shrink too. If so, the old-fashioned Regge model may turn out to be right after all!

II. B. Re f(0) AND TOTAL CROSS SECTIONS

For the more stable particles (π, K, p) we propose to measure the forward scattering down to values of $|t| = 0.001$ $(\text{GeV/c})^2$. This enables us to measure the real part of f(0) by observing the interference of the nuclear and coulomb amplitudes. These measurements extending on the high side to $|t| \cong 0.2$ or more allow a simultaneous determination of Re f(0), b and c, and σ_{tot} for the π-p and K-p interactions. The quantities b and c are the coefficients of t and t^2 in the exponential expression for the nuclear differential cross section. In the p-p case, in the absence of polarization data, an additional assumption such as spin independence is required to obtain σ_{tot}.

Crudely, the small $|t|$ region (0.-01 to 0.1) gives the ratio of Re f(0)/Im f(0) $\equiv \alpha$, the region beyond 0.1 gives

b, c and the overall magnitude of the cross section and, by extrapolation, $d\sigma/dt$ $(t = 0)$. The total cross section is then obtained via the optical theorem. Simultaneously with the measurement of $d\sigma/dt$ we intend to measure σ_{tot} by an attenuation measurement and thus provide a check of the procedures and ultimately of the optical theorem. Figure 3 shows a typical $d\sigma/dt$ for

$$\text{Re } f(0) = 0 \text{ and for Re } f(0)/\text{Im } f(0) \equiv \alpha = 0.1.$$

The real parts of $f(0)$ are of interest for two general reasons. First and most fundamentally, they allow (together with σ_{tot}) a test of the forward dispersion relations, at an energy which is an order of magnitude higher than previously available. These considerations apply in πp scattering and also for K-p scattering perhaps with an additional subtraction. Following the analysis of Oehme[3] these measurements would allow a test of microscopic causality down to distances of 10^{-16} cm to 10^{-17} cm.

From a more phenomenological point of view, Re $f(0)$ and σ_{tot} are quantities whose energy dependence is predicted by the Regge pole and other theories discussed in the previous section. Among the many possibilities we note two of some interest.

First, the possibility that the Pomeranchuk theorem is violated, i.e. that the leveling out of the Serpukhov cross sections represents an "asymptotic act" predicts that $f(0)$ at high energies become essentially real. Secondly, high energy scattering models with Pomeranchuk generated cuts predict that the asymptotic values of the total cross

sections are approached from below. On the basis of this picture one would expect all the total cross sections except $\bar{p}p$ to be rising in the NAL region! Figure 4 illustrates a typical model of this type.

For designing the experiment it is useful to estimate a reasonably pessimistic lower limit to α. We note that if the Serpukhov data are ignored and one uses the fits to the total cross section made by Lindenbaum[4] and assumes the forward dispersion relations, one finds $\alpha \approx 0.03$ to 0.05 at 150 GeV/c and $\alpha \approx 0.05$ to 0.1 at 100 GeV/c. All other calculations known to us give larger values of α. Accordingly, we have set a desired precision in α of $\Delta\alpha = 0.01$.

We turn now to some quasi-experimental considerations. For concreteness we consider πp scattering. We comment that many of the problems encountered have been considered by Foley et al.[5] in their important work on the pion-nucleon forward dispersion relations at AGS energies. Following the notation of Reference 5 we write the differential cross section:

$$\frac{d\sigma^{\pm}}{dt} = \frac{Fc^2}{t^2} \mp \frac{2Fc}{|t|} \operatorname{Im}(A_{N_{\pm}}) \left[\alpha_{\pm}\cos 2\delta \pm \sin\delta\right] + (1 + \alpha_{\pm}^2)\left[\operatorname{Im} A_{N_{\pm}}\right]^2 \qquad (1)$$

where $\pm$ refers to $\pi^{\pm}p$

F_c is the Coulomb amplitude,

$$F_c = \frac{2\sqrt{\pi}\, e^2}{\beta c} G_{Ep}\, G_{E\pi}$$

G_{Ep}, $G_{E\pi}$ are the (electric) form factors for the proton and pion respectively.

A_N is the nuclear amplitude.

α = Re A_N/Im A_N and assumed to be constant

$\delta = \frac{e^2}{\beta c} \ln \left(\frac{1.06}{pa\ \theta}\right)$

p = momentum and a is a "radius" parameter in the Gaussian fit to the form factor.

Figures 5 and 6 show typical values of $d\sigma/dt$ in the interference region. In calculating the figures we have neglected the form factor of the pion and the ct^2 term in the nuclear scattering exponential. Both are qualitatively unimportant.

To investigate the statistics needed for the experiment, we have, by well known techniques, calculated the error matrix we expect to apply after accumulating N events. Again in this calculation we have neglected the ct^2 term which will have only a small effect on the errors in α and σ_T. The result is:

Error Matrix = $\frac{1}{N}$ x

α	b	σ_T	
11.98	16.98	47.02	α
16.98	150.53	215.15	b
47.02	215.15	508.57	σ_T

Thus, to get an rms error in α of 0.01 we need about 120,000 events. Allowing for inelastic triggers we expect to require about 0.5 to 1.0 x 10^6 recorded events per measurement.

As noted in the section on experimental arrangement it is important from a systematic point of view to cover the full t range described so as to avoid problems of relative normalization.

II. C. THE HYPERCHARGE DEPENDENCE OF FORWARD SCATTERING

Our program of studying the elastic scattering of charge particles (Proposal 69 and 97) is particularly relevant to studies of the hypercharge dependence of the strong interactions, within a given family of particles. The possibilities are most striking in baryon-baryon scattering, where we will observe states with four different values of the strangeness:

p-p	$S = 0$
Σ^--p, Λ-p, (Σ^+-p)	$S = -1$
Ξ^--p, Ξ°-p	$S = -2$
Ω^--p	$S = -3$

In terms of the quark model, we have reactions containing from zero to three strange quarks. These reactions are an ideal testing ground for this model, since the simplest interpretation of present data is that the strange quark has a somewhat different interaction from the non-strange pair.

The least speculative predictions of interactions in the quark model are those dependent on the assumption of additivity of quark amplitudes for forward scattering, since the momentum transfers are then very small. The tests of this model in meson-baryon scattering are well known, and we would look forward to testing these at high energies, where secondary effects are presumably smaller. In baryon-baryon scattering, there are a host of sum rules which may be predicted. A sample of these is given below[6,7]. These are divided into groups, with succeeding groups making the stronger assumptions of spin independence, SU (3) invariance, and high energy limits on quark scattering. Particle labels denote

values of the corresponding forward scattering cross sections:

$$\Sigma^+p - \Sigma^-p = pp - np + \Xi^\circ p - \Xi^- p$$

$$\sqrt{3}\ (\Lambda p - \Sigma^\circ p) = pp - np - 1/2\ \left[\Sigma^+p - \Sigma^-p\right]$$

$$\Lambda p = 1/2\ \left[\Sigma^+p + \Sigma^-p\right]$$

$$pp + \Lambda p = np + \Sigma^+p$$

$$\Sigma^-p = \Xi^\circ p$$

$$\Sigma^+p = np$$

$$np = 1/2\ \left[\Lambda p + pp\right]$$

$$\Lambda p + \Xi^-p - 2\Sigma^-p = 3/4\ \left[np - \Sigma^+p\right]$$

$$3\ \left[2\Lambda p - \Sigma^-p\right] = 4\ np - \Sigma^+p$$

$$np = pp,\ \Lambda p = \Sigma^-p = \Sigma^+p$$

$$\Xi^-p = \Xi^\circ p$$

$$\Lambda p = 1/2\left[np + \Xi^\circ p\right]$$

Aside from the quark model, one can test the predictions of SU3 for the baryon-baryon scattering amplitudes. This is again a favorable place for a test because of small momentum transfers. One needs at least three hyperon cross sections, in addition to the nucleon cross sections, to carry out a test.

III. A. HIGH RESOLUTION DETECTORS

This experiment relies on the use of novel detectors with high spatial resolution. Since these are described only in as yet unpublished reports, a summary of the work which has been done and the characteristics of these detectors may be of interest here. Members of the team

presenting this proposal have worked on high resolution spark chambers[8,9] and high resolution proportional chambers[10]. At the present moment, the wire spark chambers have higher accuracy, and our experimental design is based on the resolution which can be achieved in this way with the techniques we have demonstrated. This resolution, 50 μ, is about five to ten times better than that usually achieved in wire spark chambers.

A parallel effort in proportional chambers is yielding very encouraging results. We are confident of achieving an effective resolution within a factor of three of the above value with the present techniques, and we may reasonably hope for further improvements in the near future. Our plan for this experiment is to prepare the wire spark chambers which we know will provide the resolution needed, but to pursue the proportional chamber development as well. If the latter turn out to meet the resolution requirement, we would certainly adopt them to gain the advantage of a factor of a hundred or more in rate and much better time resolution.

The improvement in the performance of the wire spark chamber resolution derives from a program which attacks each of the primary limitations in wire spark chamber accuracy. The diffusion of electrons in the spark chamber gas, the basic limitation, is reduced by increasing the gas pressure. The effect of structure and instabilities of the spark column is reduced by reducing the gap width, and thus the spark length. This is permissible because of the higher pressure, which increases the number of ions per unit length, and reduces the spark formation time. Reducing the gap width

also decreases the effects of track inclination to the spark chamber plane. In using magnetostrictive readout, the resolution is improved by reducing the size of magnetostrictive wire in the pick-up coil, and by providing a scale magnification by fanning out the wires to four times larger spacing at the readout line.

The wire planes which have been used so far are eteched from 10 μm copper on a Kapton backing, with a spacing of eight wires per millimeter. A spacing of twelve wires per millimeter is also feasible with the same technique. The chamber is operated at a pressure of 5-15 atmospheres of 90% neon, 10% helium, 1% argon, 0.1% CH_4. A set of these chambers 4 x 4 cm^2 has been operated in a low energy test beam to measure the resolution. The results, which were limited by multiple scattering, gave an upper limit on the resolution of 65 μm (1 standard deviation limit). It should be possible to attain 25 μm resolution with these chambers. In gases at reasonable pressures, diffusion sets the ultimate resolution limit at 10-15 μm.

The developments in proportional chambers have so far relied on careful field shaping and the possibility of variable pressure[10]. Chambers have been operated with a spacing of one and two wires per millimeter. Both chambers operate well, and the former has been operated in a test beam, with demonstrated efficiency and resolution. With a pair of staggered chambers, this promises 125 μm resoltuion. Further development is continuing steadily, and within a few months we should know if it is possible to produce proportional chambers of the required resoltuion at the date needed for this experiment.

III. B. ANGULAR AND MOMENTUM RESOLUTION REQUIREMENTS

We wish to measure elastic scattering at energies up to 200 GeV, with an accuracy in momentum transfer which allows the measurement of the angular range in which Coulomb single scattering is dominant, in an experiment which covers the diffraction peak. In a 0.5 m hydrogen target, this is the transverse momentum range from ~ 30 MeV/c to ~ 60 MeV/c. Smaller transverse momenta are dominated by plural scattering, larger by nuclear scattering (see Figure 3).

One potential limitation is the multiple scattering in the pair of detectors on the upstream and downstream ends of the hydrogen target. Each unit will contain three x-y spark planes, or a total of six, together with the neon gas and chamber windows. The average transverse momentum due to multiple scattering imparted by the whole assembly is 3.0 to 4.0 MeV/c, depending on design details affecting the length of gas, etc. This turns out to be the same as the multiple scattering in the hydrogen target of ~ 1/2 meter length, and is much smaller than the lower end of the range of transverse momenta in scattering in the range to be measured. The plural scattering in the detector is important up to ~ 25 MeV/c, but most of this will be removed in the analysis since the space resolution of the chambers is sufficient to distinguish whether the origin of scatters of more than 15 MeV/c is in the detector or in the target. In short, the scattering in the detector does not limit this aspect of the experiment.

The lever arm needed to equal the error due to scattering is calculated assuming two pairs of detectors on either side of the target, each separated by length L. Each detector is assumed to provide two measurements of each coordinate, with resolutions of 50 μm. The error in scattering angle is then $\sqrt{2}$ x 50 μm/L, and the corresponding transverse momentum for a particle of momentum 200 GeV/c is

$$P_\perp = 2 \times 10^5 \times \sqrt{2} \times 50 \times 10^{-6}/L$$
$$= 14 \text{ MeV/c/L}$$

The length needed to give $P_\perp$ = 3.5 MeV/c is 4 m.

The momentum of the incoming particle is measured from the properties of the beam and its position at the appropriate location. The momentum of the outgoing particle is measured by the decay spectrometer, in the case of the short lived particles, and by deflection in a bending magnet in the case of the long lived particles. In the latter case, the multiple scattering is the limitation of the accuracy:

$$\frac{\Delta p}{p} = \frac{P_\perp \text{ due to multiple scattering}}{P_\perp \text{ due to bending magnet}}$$

We propose to use two standard 20 foot NAL main ring magnets at 20 kG, which gives $P_\perp$ = 7200 MeV/c, and thus $\Delta p/p$ = 0.05%. The highest momentum particles from inelastic processes differ from elastically scattered particles by 0.07% at 200 GeV/c.

III. C. LONG LIVED PARTICLE EXPERIMENTAL ARRANGEMENT

The short lived particles can be identified by their decays, thereby easing the problem of the mass identifying

Cerenkov counter. The identification of the more stable particles must rely on the operation of refined Cerenkov counters. For this and other reasons it is desirable to perform this part of the experiment in the high resolution 2.5 mr beam. The layout is shown in Figure 7.

The angle of the particle is measured before and after the 1/2 meter hydrogen target by small high resolution detectors. The momentum of the scattered particle is measured by the deflection in two accelerator magnets. The lever arms are set by the considerations discussed in the section on Angle and Momentum Resolution, taking into account the experimental details. For example, the lever arm after the magnet is made larger because the final chamber is somewhat larger, about 10 cm, than those near the target, and may not display the same accuracy we have achieved in our 4 cm chambers.

The excess drift space near the target is provided so that we can distinguish scatters in the hydrogen target from those in the adjacent detectors, and thereby eliminate that source of background from the final data. Our resolution implies an accuracy of < 0.7 m in the longitudinal position of the scattering at the smallest scattering we would contemplate analyzing, a transverse momentum of 15 MeV/c.

The trigger is defined by suitable Cerenkov signals, location of the particle at the dispersive focus of the beam, the defining counters immediately preceding the first spark chamber, S_1, and no count in the 2 mm veto counter between the two magnets. The incident beam, with a focal spot $\sim$ 0.9 mm

in diameter[11], is focused on this counter. The dispersion due to the preceding magnet, for $\Delta p/p = 1\%$ is 0.7 mm. If it is necessary to decrease the solid angle or momentum bite of the beam, to maintain the ideal focal spot diameter, the larger solid angle of our apparatus allows this to be done with little or no sacrifice in data rate.

The hydrogen target is surrounded by a proton detector. Although the detection of the proton is not required, its observation will be used as a check, in those events in which it has enough momentum to escape the target.

The transverse momentum range accepted through the apparatus is just under 1 GeV/c for 200 GeV/c incident or 250 MeV/c for 50 GeV/c incident. This means that over the whole region of interest one can observe a large portion of the diffraction peak without disturbing any of the equipment. We believe that this is very important in avoiding systematic errors in the Coulomb interference and diffraction peak shrinkage experiments. To cover this range of $|t|$ with conventional detectors would require a very large investment in magnets.

IV. SUMMARY OF RATES AND BEAM REQUIREMENTS

Coulomb Interference Measurements with Stable Particles

In this case data taking will be limited by the dead time of the apparatus. This is easily seen given that the effective cross section is $\approx$ 1-2 mb for elastic events or about one event every 300 to 600 beam particles. Typical π fluxes available are $\approx 10^5$ per pulse and K fluxes are 10^3 to 10^4 per pulse. Furthermore, we have assumed that only

about 1/8 of all triggers are true elastics. Thus assuming a 1 sec spill and a 10 ms spark chamber dead time we expect about 12 elastics per pulse.

As argued previously, about 10^5 elastics are needed for each measurement point (i.e., particle and momentum) to give an error in α = Re f(0)/Im f(0) of 0.01. This amounts to about 10 hours per measurement.

We would propose a measurement matrix of π^+, π^-, K^+, K^-, p and $\bar{p}$ each at three energies, giving a total of 180 (ideal) hours for this phase of the experiment. Obviously, if the precision proportional chamber development is successful the time required will be less by an order of magnitude.

Experimental Equipment Required

Much of the counting and data collecting equipment required for the experiment is very similar to that being developed by this group for the BNL hyperon experiment. We will require an on-line data collecting computer such as the NAL PDP-15 which will be used for the BNY hyperon experiment. The interfaces being developed for its BNL usage would also be needed for this experiment, and it is requested that this same machine be made available to us. Ideally, as in our BNL usage, we would like a link from the PDP-15 to a larger machine capable of carrying some fraction of the data through to the final analysis. However, if this is not available, access to a larger on-site computer which would be capable of reading the magnetic tape output of the PDP-15 would be essential.

The long lived particle phase requires a beam of good momentum resoltuion and most importantly of optical quality such that Cerenkov counters capable of distinguishing π, K, and p from each other could be incorporated into it. It must be capable of a focal spot of about 1 mm in diameter. Two NAL main ring magnets are used for the momentum analysis of the scattered particles.

References

[1] T. T. Chou and C. N. Yang, Phys. Rev. 170, 1591 (1968).

[2] L. Durand and R. Lipes, Phys. Rev. Letters 20, 637 (1968).

[3] R. Oehme, Phys. Rev. 100, 1503 (1955).

[4] S. J. Lendenbaum, "Pion-Nucleon Scattering," Wiley Interscience 1969, edited by G. L. Shaw and D. Y. Wong, p. 111.

[5] K. J. Foley, et al., Phys. Rev. Letters 19, 193 (1967).

[6] D. A. Akyeampong, Nuovo Cimento 48A, 519 (1967).

[7] Dare, Nuovo Cimento 52A, 1015 (1967).

[8] W. J. Willis, W. Bergmann, and R. Majker, "High Resolution Optical Spark Chamber," (to be submitted to Nuclear Instruments and Methods).

[9] W. J. Willis and I. J. Winters, "High Resolution Wire Spark Chambers," (ibid).

[10] M. Atac and J. Lach, "High Spatial Resolution Proportional Chambers," NAL Report FN-208, April 1970.

[11] D. Reeder and J. MacLachlan, 1969 Summer Study, NAL Vol. 1, p. 41.

Figure 1

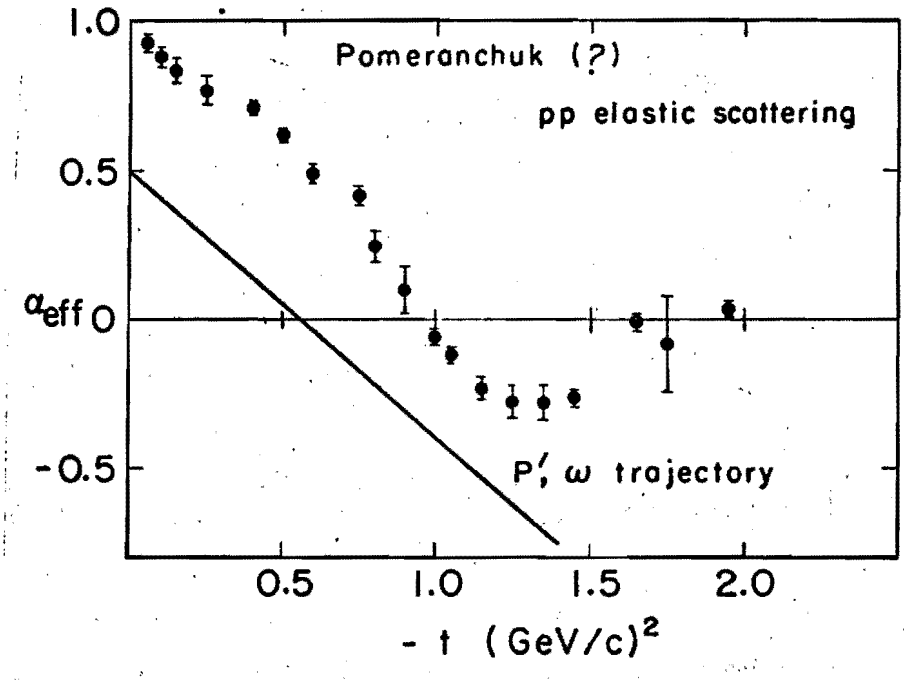

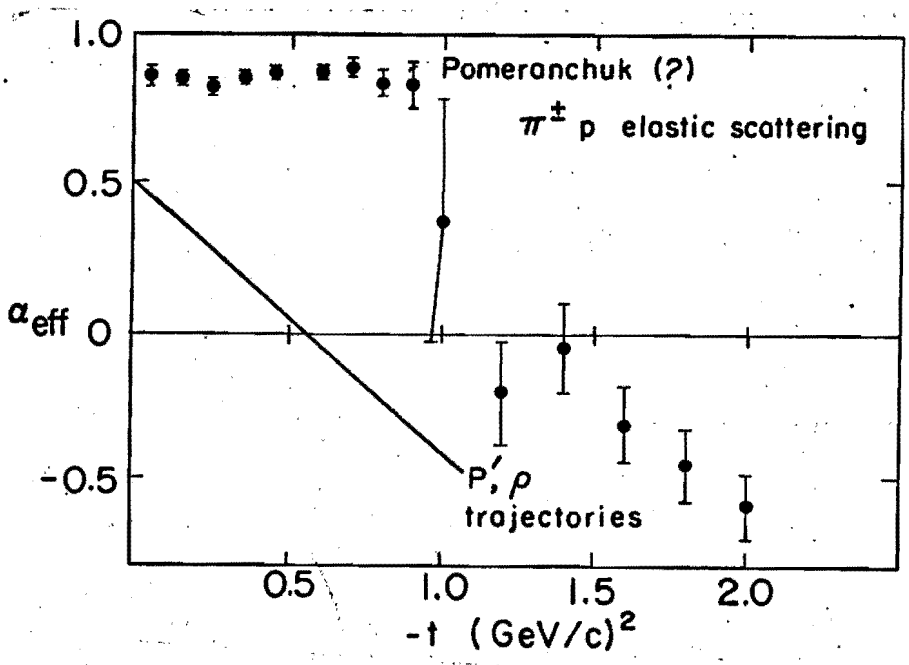

From; G. Fox, High Energy Collisions

Figure 2

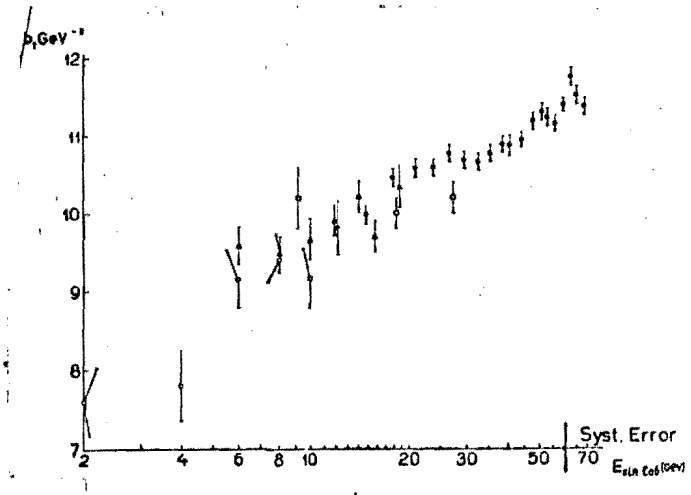

The slope parameter b_1 from elastic proton-proton collisions (see text) as a function of energy. The symbols represent data from Ref. 14, Ref. 16, Ref. 17 and Ref. 18.

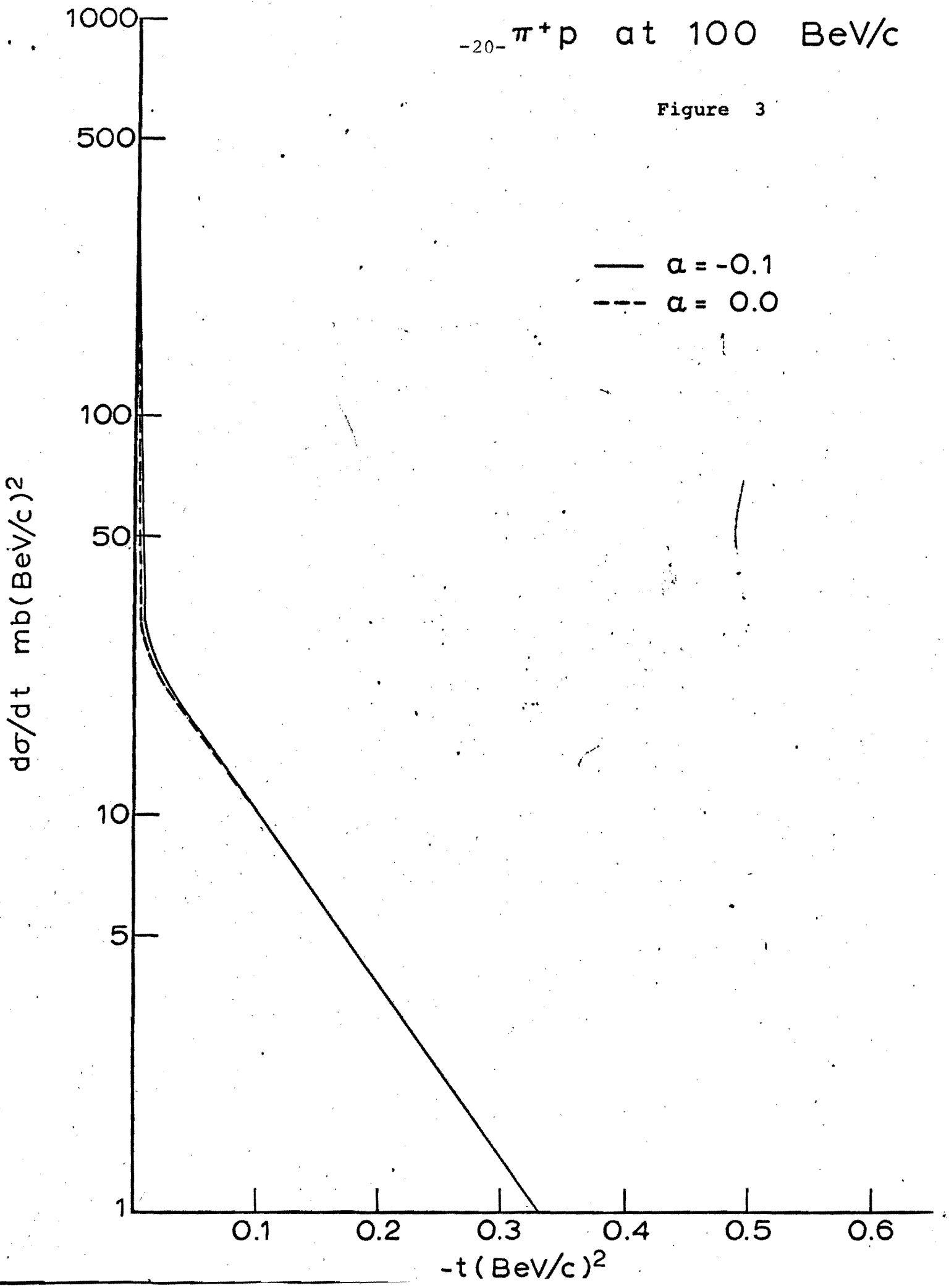
$\pi^+ p$ at 100 BeV/c
Figure 3
a = -0.1
a = 0.0
1000
500
100
50
10
5
1
dσ/dt mb(BeV/c)²
0.1
0.2
0.3
0.4
0.5
0.6
-t (BeV/c)²

Figure 4

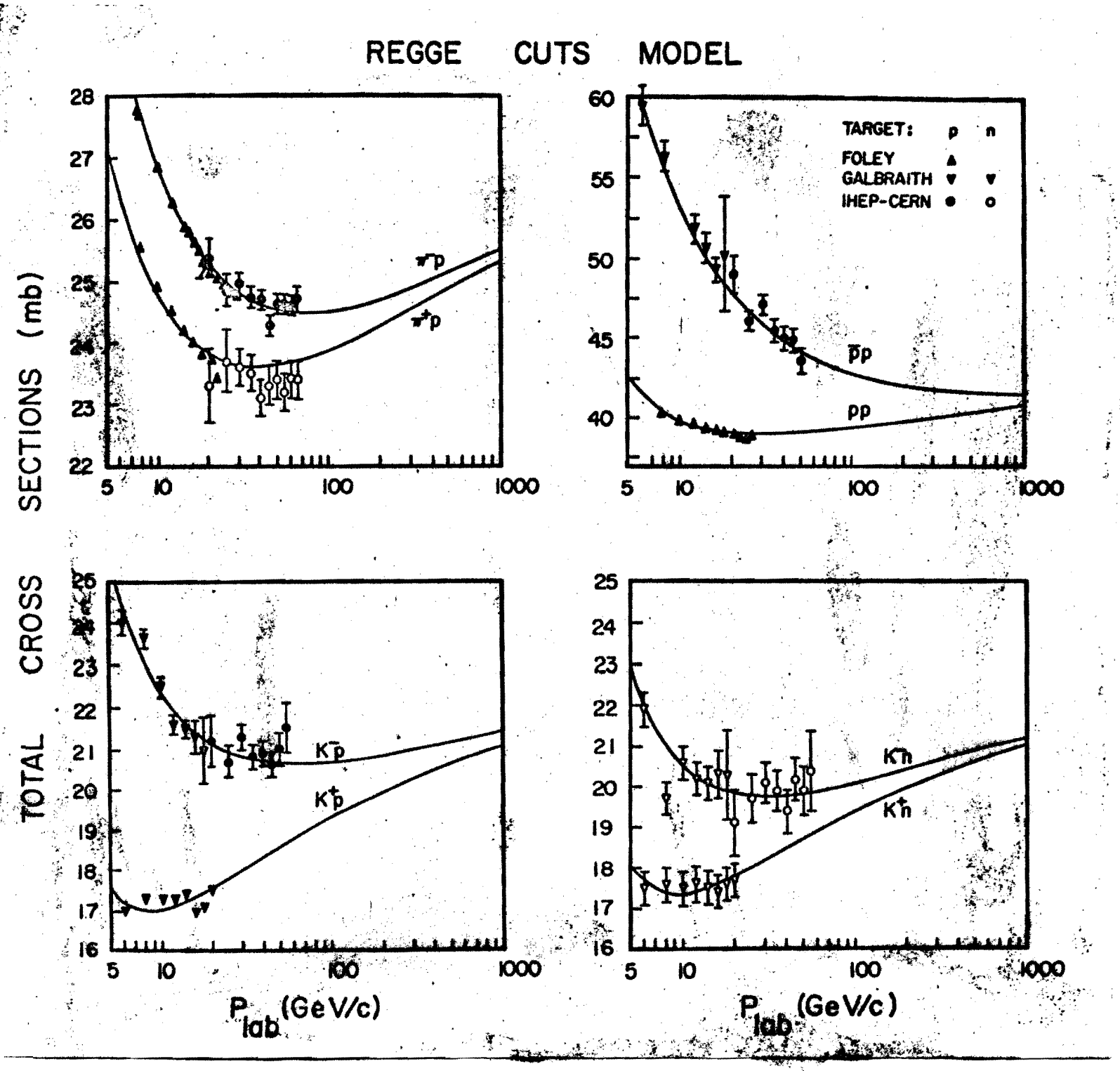
REGGE CUTS MODEL
TOTAL CROSS SECTIONS (mb)
TARGET: p n
FOLEY
GALBRAITH
IHEP-CERN
π⁻p
π⁺p
p̄p
pp
K⁻p
K⁺p
K⁻n
K⁺n
P lab (GeV/c)
P lab (GeV/c)

Figure 5

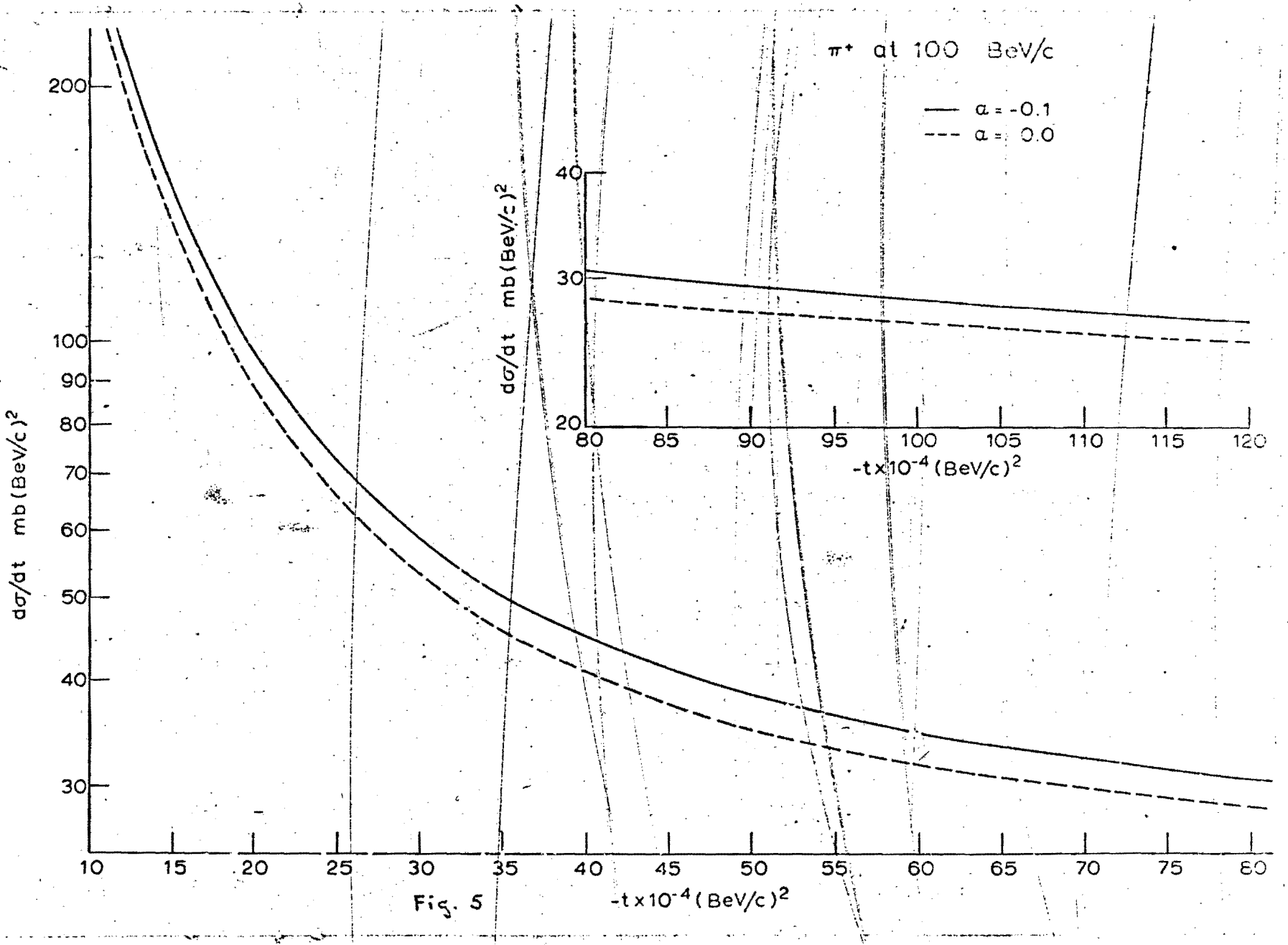

Fig. 5

Figure 6

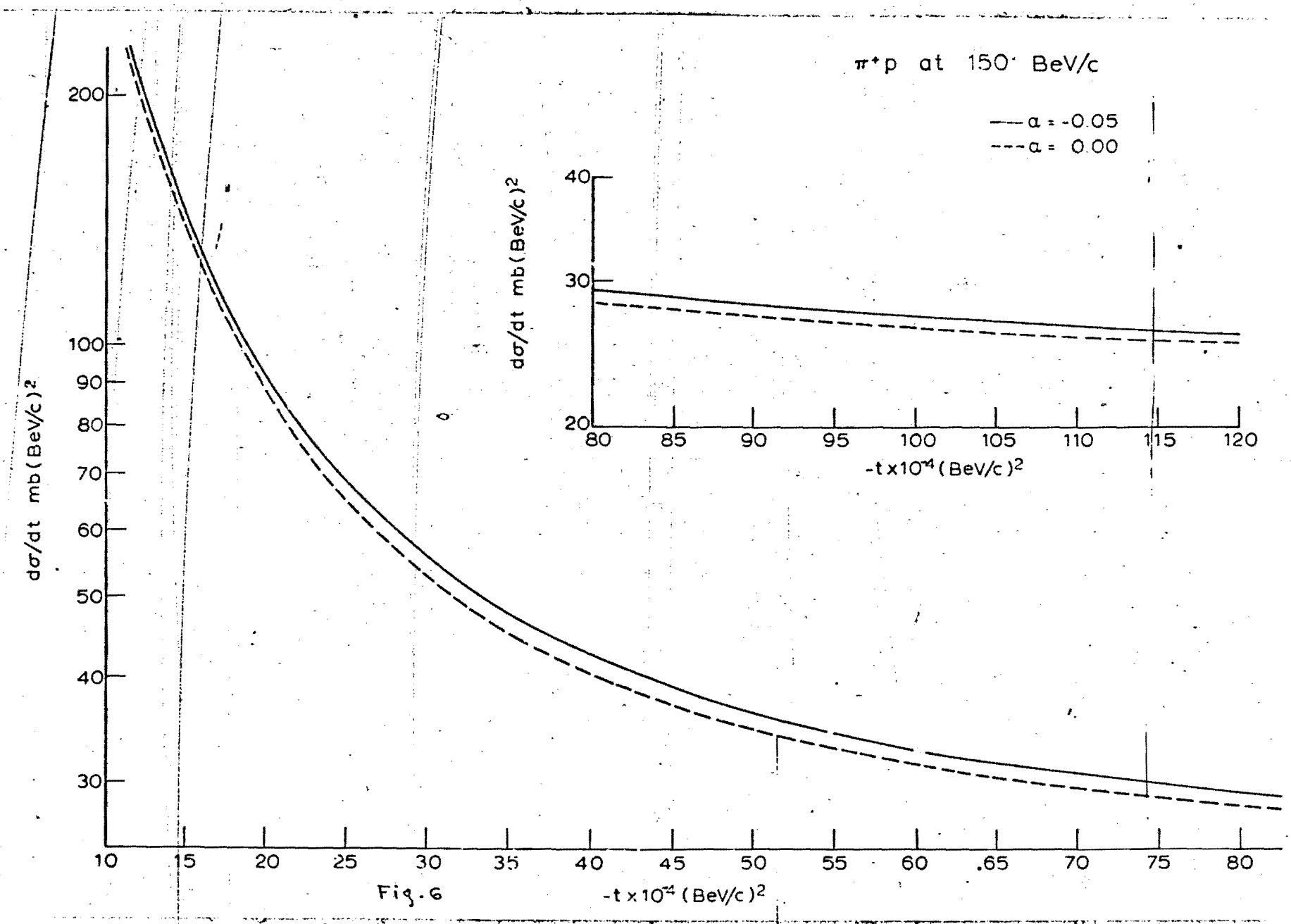

Fig. 6

Figure 7

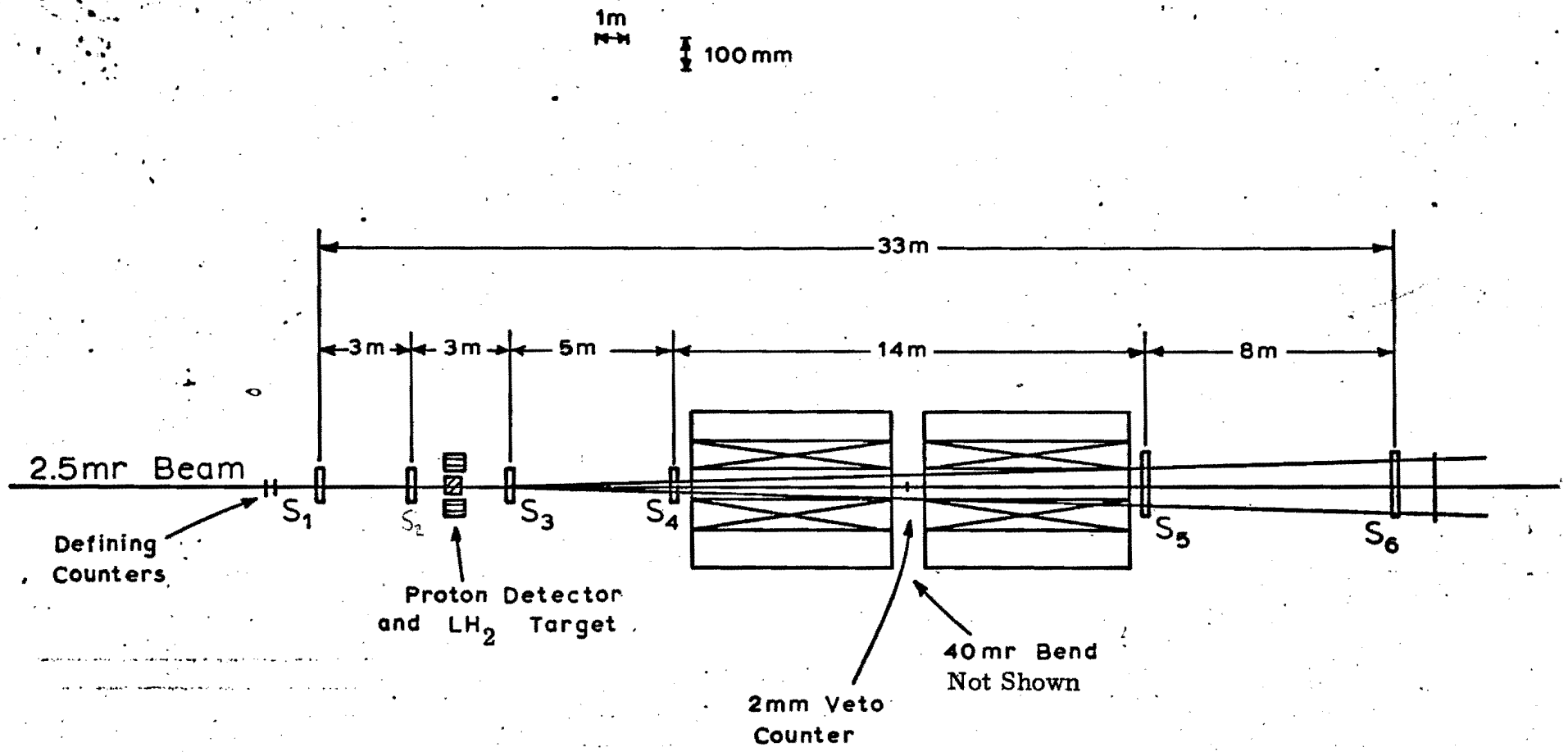

LONG-LIVED HADRON LAYOUT